Journal of Statistical Mechanics:
Theory and Experiment

SISSA

PAPER

# Exclusion volumes of convex bodies in high space dimensions: applications to virial coefficients and continuum percolation

To cite this article: Salvatore Torquato and Yang Jiao *J. Stat. Mech.* (2022) 093404

View the article online for updates and enhancements.




IOP ebooks™

Bringing together innovative digital publishing with leading authors from the global scientific community.

Start exploring the collection–download the first chapter of every title for free.

This content was downloaded from IP address 137.83.217.149 on 21/09/2022 at 14:02

Journal of Statistical Mechanics: Theory and Experiment
An IOP and SISSA journal

PAPER: Interdisciplinary statistical mechanics

# Exclusion volumes of convex bodies in high space dimensions: applications to virial coefficients and continuum percolation

**Salvatore Torquato**[1,2,3,4,*] **and Yang Jiao**[5,6]

[1] Department of Chemistry, Princeton University, Princeton, NJ 08544, United States of America
[2] Department of Physics, Princeton University, Princeton, NJ 08544, United States of America
[3] Princeton Institute of Materials, Princeton University, Princeton, NJ 08544, United States of America
[4] Program in Applied and Computational Mathematics, Princeton University, Princeton, NJ 08544, United States of America
[5] Materials Science and Engineering, Arizona State University, Tempe, AZ 85287, United States of America
[6] Department of Physics, Arizona State University, Tempe, AZ 85287, United States of America
E-mail: torquato@electron.princeton.edu

Received 5 April 2022
Accepted for publication 14 August 2022
Published 21 September 2022

Online at stacks.iop.org/JSTAT/2022/093404
https://doi.org/10.1088/1742-5468/ac8c8b

**Abstract.** Using the concepts of mixed volumes and quermassintegrals of convex geometry, we derive an exact formula for the exclusion volume $v_{\rm ex}(K)$ for a general convex body $K$ that applies in any space dimension. While our main interests concern the rotationally-averaged exclusion volume of a convex body with respect to another convex body, we also describe some results for the exclusion volumes for convex bodies with the same orientation. We show that the sphere minimizes the dimensionless exclusion volume $v_{\rm ex}(K)/v(K)$ among all convex bodies, whether randomly oriented or uniformly oriented, for any $d$, where $v(K)$ is

*Author to whom any correspondence should be addressed.

© 2022 IOP Publishing Ltd and SISSA Medialab srl
1742-5468/22/093404+38$33.00

the volume of $K$. When the bodies have the same orientation, the simplex maximizes the dimensionless exclusion volume for any $d$ with a large-$d$ asymptotic scaling behavior of $2^{2d}/d^{3/2}$, which is to be contrasted with the corresponding scaling of $2^d$ for the sphere. We present explicit formulas for quermassintegrals $W_0(K), \ldots, W_d(K)$ for many different nonspherical convex bodies, including cubes, parallelepipeds, regular simplices, cross-polytopes, cylinders, spherocylinders, ellipsoids as well as lower-dimensional bodies, such as hyperplates and line segments. These results are utilized to determine the rotationally-averaged exclusion volume $v_{\rm ex}(K)$ for these convex-body shapes for dimensions 2 through 12. While the sphere is the shape possessing the minimal dimensionless exclusion volume, we show that, among the convex bodies considered that are sufficiently compact, the simplex possesses the maximal $v_{\rm ex}(K)/v(K)$ with a scaling behavior of $2^{1.6618\ldots d}$. Subsequently, we apply these results to determine the corresponding second virial coefficient $B_2(K)$ of the aforementioned hard hyperparticles. Our results are also applied to compute estimates of the continuum percolation threshold $\eta_{\rm c}$ derived previously by the authors for systems of identical overlapping convex bodies. We conjecture that overlapping spheres possess the maximal value of $\eta_{\rm c}$ among all identical nonzero-volume convex overlapping bodies for $d \geqslant 2$, randomly or uniformly oriented, and that, among all identical, oriented nonzero-volume convex bodies, overlapping simplices have the minimal value of $\eta_{\rm c}$ for $d \geqslant 2$.

**Keywords:** percolation problems, random/ordered microstructures, series expansions

## Contents

**1. Introduction ..... 3**

**2. Basic definitions and background ..... 6**

2.1. Exclusion zones ..... 6
2.2. Exclusion volume averaged over all rotations ..... 7
2.3. Quermassintegrals and mixed volumes ..... 7

**3. General formula for the rotationally-averaged exclusion volume ..... 8**

3.1. Exclusion volume ..... 8
3.2. Quermassinegrals as cross-sectional volumes ..... 9

**4. Determination of quermassintegrals for specific convex bodies in $\mathbb{R}^{\rm d}$. . . 12**

4.1. Spheres ..... 13
4.2. Cube ..... 13
4.3. Right parallelepiped ..... 14
4.4. Right parallelepiped with a specific aspect ratio ..... 14
4.5. Convex cylinder ..... 14
4.6. Spherocylinder ..... 15
4.7. General ellipsoid ..... 15

J. Stat. Mech. (2022) 093404

4.8. Ellipsoid of revolution ..... 16
4.9. Regular simplex ..... 16
4.10. Cross-polytope ..... 16
4.11. Spherical hyperplates ..... 17
4.12. Cubical hyperplates ..... 17
4.13. Line segment ..... 18
**5. Extremal values for exclusion volumes of oriented and non-oriented bodies ..... 18**
5.1. Oriented exclusion volume ..... 19
5.2. Extremal exclusion volumes for oriented hyperparticles ..... 19
5.3. Extremal exclusion volumes for non-oriented hyperparticles ..... 20
**6. Results ..... 21**
6.1. Dimensionless exclusion volumes across dimensions ..... 21
6.2. Dimensionless second virial coefficients across dimensions ..... 24
6.3. Percolation thresholds across dimensions ..... 25
**7. Conclusions ..... 30**
**Acknowledgments ..... 32**
**Appendix A. Quermassintegrals of lower-dimensional bodies and hyperplates ..... 32**
A.1. Intrinsic volumes ..... 33
A.2. Application to spherical hyperplates ..... 34
A.3. Application to cubical hyperplates ..... 35
A.4. Dimensionless exclusion volume for selected shapes across dimensions ..... 35
**References ..... 37**

## 1. Introduction

The exclusion volume of an arbitrary $d$-dimensional convex body (hyperparticle) $K$ in $d$-dimensional Euclidean space $\mathbb{R}^d$ is a fundamental quantity that arises in the virial expansion of the pressure of a hard-hyperparticle fluid [1–4], estimates of continuum percolation thresholds [5–9] and a variety of problems involving the distance of closest approach of two nonoverlapping bodies [10–15]. The exclusion volume is the region of space that is excluded to one hyperparticle due the presence of another one with a specific relative orientation. Whereas in the case of hyperspheres or *oriented* centrally-symmetric hyperparticles (e.g. cubes or cross-polytopes), the exclusion volume relative to the volume of the convex body $K$, $v(K)$, is simply equal to $2^d$, its determination for general convex bodies with arbitrary relative orientations is nontrivial. The generalized exclusion volume $v_{\rm ex}(K)$ of a convex body $K$ can be expressed as



J. Stat. Mech. (2022) 093404

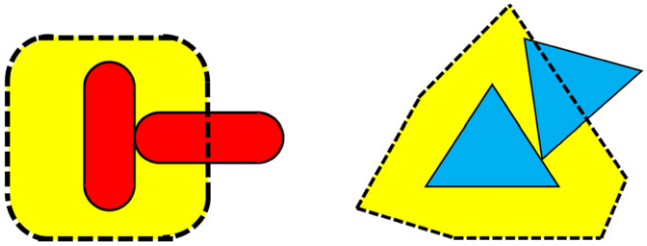


**Figure 1.** Illustration of the exclusion volume of two-dimensional convex bodies with a fixed orientation with respect to one another. In each of the two examples, the exclusion volume is the region interior to the boundary delineated by the dashed lines. (Left) Centrally symmetric spherocylinder. (Right) Non-centrally symmetric equilateral triangle (two-dimensional regular simplex).

$$v_{\rm ex}(K) = \int_{\mathbb{R}^d} f(\mathbf{r}, \boldsymbol{\omega}\,; K) p(\boldsymbol{\omega}\,; K) \mathrm{d}\mathbf{r}\, \mathrm{d}\boldsymbol{\omega}, \tag{1}$$

where $f(\mathbf{r}, \boldsymbol{\omega}\,;\ K)$ is the exclusion-region indicator function [7, 9], $\mathbf{r}$ and $\boldsymbol{\omega}$ is the centroid position and orientation of one body, respectively, with respect to a coordinate system at the centroid of the other body with some fixed orientation, and $p(\boldsymbol{\omega}\,;\ K)$ is the orientational probability density function. Figure 1 depicts two-dimensional examples of exclusion volumes for a centrally symmetric body and noncentrally symmetric body.

In this paper, we derive exact general expressions for the exclusion volume $v_{\rm ex}(K)$ of a convex body $K$ for any dimension in terms of the concepts of quermassintegrals and mixed volumes of convex geometry [16–19]. While we mainly treat the rotationally-averaged exclusion volume of a convex body with respect to another convex body, we also describe some results for the exclusion volumes for convex bodies with the same orientation. We then provide explicit formulas for quermassintegrals for specific nonspherical convex bodies, including cubes, cylinders, spherocylinders, parallelepipeds, regular simplices, cross-polytopes, ellipsoids as well as lower-dimensional bodies, such as hyperplates and line segments. These results are employed to determine the rotationally-averaged exclusion volume for these specific convex-body shapes for dimensions 2 through 12. Note that the three regular polytopes considered here (cube, regular simplex and cross-polytope) are the only regular polytopes possible for $d \geqslant 5$ [20].

Subsequently, we apply these results to determine the corresponding second virial coefficient $B_2(K)$ that arises in the virial expansion of the pressure $P$ of hard-particle fluids composed of such shapes through second order in the density [3], namely,

$$\frac{P}{k_{\rm B}T} = \rho + \rho^2 B_2(K) + \mathcal{O}(\rho^3), \tag{2}$$

where $\rho$ is the number density, i.e. the number of convex bodies per unit volume in the thermodynamic limit, $k_{\rm B}$ is the Boltzmann constant, $T$ is absolute temperature, and

$$B_2(K) = \frac{1}{2} v_{\rm ex}(K). \tag{3}$$



J. Stat. Mech. (2022) 093404

It is noteworthy that third- and higher-order terms in the viral expansion (2) of a hard-particle fluid become negligibly small in the high-$d$ asymptotic limit [21]. The exclusion volume arises at the second virial level due to the nonoverlap constraint of two convex bodies when they come in contact with one another. While $B_2(K)$ has long been known for a variety of nonspherical hard particles in two and three dimensions [1], no such results appear to have been obtained for $d \geqslant 4$ until the present work. We shall also apply our results to compute estimates of the continuum percolation threshold $\eta_c$ derived by Torquato and Jiao [9] for systems of identical *overlapping* convex bodies with arbitrary orientational distributions in $d$-dimensional Euclidean space $\mathbb{R}^d$ that depend on the exclusion volume $v_{ex}(K)$, which arises here because it defines the region when two hyperparticles overlap [9]. In particular, they derived the following lower bound on the percolation threshold $\eta_c$ that is applicable for any $d$:

$$\eta_c \geqslant \frac{v(K)}{v_{ex}(K)}, \tag{4}$$

where $\eta = \rho v(K)$ is a dimensionless (reduced) density. The inequality (4) applies in all dimensions, becomes sharper as dimension increases, and exact in the limit $d \to \infty$ [9]. Torquato and Jiao [9] conjectured the following sharper scaling relation to estimate $\eta_c$:

$$\eta_c \approx \frac{(\eta_c)_S}{(v/v_{ex})_S}\left(\frac{v(K)}{v_{ex}(K)}\right) = 2^d\left(\frac{v(K)}{v_{ex}(K)}\right)(\eta_c)_S, \tag{5}$$

where $(\eta_c)_S$ and $(v_{ex}/v)_S = 2^d$ are the percolation threshold and dimensionless exclusion volume, respectively, for a *reference system* of overlapping hyperspheres in dimension $d$. (See [8] for accurate estimates of $(\eta_c)_S$, see [22] for $d = 2$, see [23, 24] for $d = 3$ and see [8] for $d = 4$–11.) It is noteworthy that the scaling relation (5) becomes exact in the high-$d$ limit [9]. The aforementioned counter-intuitive relationship between equilibrium hard-hyperparticle fluids and the continuum percolation model of the same overlapping hyperparticles is a consequence of a *duality* relation identified in [7], the fundamental and practical consequences of which are discussed in section 7.

The bound (4) applies for a convex body with nonzero volume ($v(K) > 0$). However, it can be generalized to apply to an overlapping systems of zero-volume convex $(d-1)$-dimensional 'hyperplates' $K_H$ in $\mathbb{R}^d$ at number density $\rho$ by replacing $v(K)$ with an appropriate 'effective volume' $v_{eff}(K_H)$ in order to define a reduced density $\eta = \rho v_{eff}(K_H)$ for hyperplates, namely, that of a $d$-dimensional sphere of radius $r$, i.e.

$$v_{eff}(K_H) = \frac{\pi^{d/2}}{\Gamma(d/2+1)} r^d, \tag{6}$$

where $\Gamma(x)$ is the Euler-gamma function and $r$ is a characteristic length scale of the hyperplate. Specifically, we choose $r$ to be the radius of a spherical hyperplate that possesses the same volume of a general hyperplate $K_H$. The scaling relation for the threshold of a hyperplate corresponding to (5) was proposed to be [9]

$$\eta_c \approx \left(\frac{v_{ex}}{v_{eff}}\right)_{SHP}\left(\frac{v_{eff}(K_H)}{v_{ex}(K_H)}\right)(\eta_c)_{SHP}, \tag{7}$$



J. Stat. Mech. (2022) 093404

where $(v_{\rm ex}/v_{\rm eff})_{\rm SHP}$ and $(\eta_{\rm c})_{\rm SHP}$ are, respectively, the dimensionless exclusion volume and percolation threshold of a reference system of overlapping spherical hyperplates, and $v_{\rm eff}(K_{\rm H})$ is given by (6).

We begin by providing basic definitions of the exclusion volume of a convex body in any dimension and the closely related concepts of mixed volumes and quermassintegrals (section 2). Using these tools from convex geometry, we then obtain a general formula for the exclusion volume of a convex body $K$ that relates $v_{\rm ex}(K)$ to the corresponding quermassintegrals (section 3). In section 4, we obtain explicit formulas for quermassintegrals for the variety of specific hyperparticles described above. Then, we describe results for the exclusion volume for oriented hyperparticles that generally do not possess central symmetry and their corresponding extremal values (section 5). Section 6 reports results for the dimensionless exclusion volume $v_{\rm ex}(K)/v(K)$ for the aforementioned specific convex-body shapes for dimensions 2 through 12. These findings are then applied to compute the corresponding second virial coefficients and estimates of the continuum percolation thresholds. In section 7, we close with concluding remarks, including the fundamental and practical implications of our results.

## 2. Basic definitions and background

We begin by defining the exclusion zones and then exclusion volume for the case of convex bodies in $\mathbb{R}^d$ over all orientations. Then, we define the key related concepts of mixed volumes and quermassintegrals.

### 2.1. Exclusion zones

Let $K, L \subset \mathbb{R}^d$ be convex bodies (compact nonempty convex sets). The sets $K$ and $L$ can be added via the operation of *Minkowski addition*:

$$K + L := \{x + y : x \in K, y \in L\} \tag{8}$$

and a set $K$ can be multiplied by the scalar $\lambda \in \mathbb{R}$, so that

$$\lambda K := \{\lambda x : x \in K\}. \tag{9}$$

For example, if $L = B_d$, where $B_d$ is the unit ball or sphere in $\mathbb{R}^d$, then for $\varepsilon \geqslant 0$, $K + \varepsilon B_d$ is the $\varepsilon$-neighborhood of $K$; see figure 2 for an illustration of this concept.

With this notion of addition, we define the exclusion zone of $K$ with respect to $L$, denoted by $Z(K, L)$, as the set of points $x$ in $\mathbb{R}^d$ such that if the centroid of $L$ were positioned at $x$, then $K$ and $L$ would intersect:

$$Z(K, L) := \{x \in \mathbb{R}^d : K \cap (L + x) \neq \emptyset\}. \tag{10}$$

A useful alternate expression for $Z(K, L)$, which will be more useful in calculations, is the following:

$$Z(K, L) = K - L = \{x - y : x \in K, y \in L\}. \tag{11}$$



J. Stat. Mech. (2022) 093404

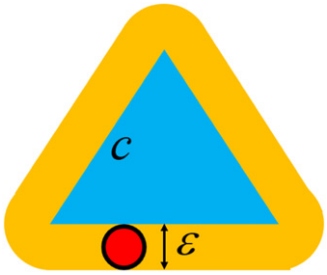



**Figure 2.** Two-dimensional illustration of the parallel body at a distance $\varepsilon$ associated with an equilateral triangle (two-dimensional simplex) of side length $c$, which is the union of the blue (or dark gray) and yellow (or light gray) regions.

To show this, suppose $x \in Z(K, L)$. Then $K \cap (L + x)$ is nonempty, so that there is $y \in K$ and $z \in L$ such that $y = x + z$: it follows that $x = y - z \in K - L$, and since $x$ was arbitrary we deduce that $Z(K, L) \subset K - L$. Conversely, suppose that $x \in K - L$. Then for $y \in K$ and $z \in L$ we have $x = y - z$, so that $y = z + x \in L + x$. Thus $y \in K \cap (L + x)$ so that $K \cap (L + x) \neq \emptyset$, meaning that $x \in Z(K, L)$ and $K - L \subset Z(K, L)$. Thus $Z(K, L) = K - L$.

### 2.2. Exclusion volume averaged over all rotations

Let $\mathrm{Vol}(Z(K, L))$ denote the volume of the exclusion zone $Z(K, L)$ associated with the bodies $K$ and $L$. We define the *rotationally-averaged exclusion volume* of a convex body $K$ with respect to another convex body $L$, denoted $v_{\mathrm{ex}}(K, L)$, to be the volume of $Z(K, L)$ averaged over all rotations of $L$ with the orientation of $K$ fixed. Let $SO(d)$ denote the set of $d$-dimensional rotations endowed with a Haar measure $\omega$, under which all rotations are equiprobable. The rotationally-averaged exclusion volume is given by

$$v_{\mathrm{ex}}(K, L) = \int_{SO(d)} \mathrm{Vol}(K + \boldsymbol{\omega} L)\, \mathrm{d}\boldsymbol{\omega}. \tag{12}$$

Notice that when $K = L$, this formula reduces to relation (1) for $v_{\mathrm{ex}}(K)$ when the orientational probability density function $p(\boldsymbol{\omega}\,;\ K)$ is set equal to unity.

### 2.3. Quermassintegrals and mixed volumes

In order to calculate the rotationally-averaged exclusion volume $v_{\mathrm{ex}}(K, L)$, we need to first employ the notion of the mixed volume. Remarkably, the volume of an $\varepsilon$-neighborhood of a convex body $K$ varies as a polynomial in $\varepsilon$ of degree $d$ [17, 18, 25], namely,

$$\mathrm{Vol}(K + \varepsilon B_d) = \frac{1}{\kappa_d} \sum_{i=0}^{d} \binom{d}{i} W_i(K) \varepsilon^i \tag{13}$$



J. Stat. Mech. (2022) 093404

where the coefficients $W_0(K), \ldots, W_d(K)$ are called *quermassintegrals* (also known as Minkowski functional or *intrinsic volumes* with a different normalization), and

$$\kappa_d = \frac{\pi^{d/2}}{\Gamma(1+d/2)} \tag{14}$$

is the volume of a unit sphere. This is the famous Steiner formula, which is a special case of the following formula:

$$\mathrm{Vol}(t_1 K_1 + \cdots + t_m K_m) = \sum_{i_1,\ldots,i_d=1}^{m} V(K_{i_1}, \ldots, K_{i_m}) t_{i_1} \ldots t_{i_m}, \tag{15}$$

where the coefficients $V(K_{i_1}, \ldots, V_{i_m})$ are called *mixed volumes* of the convex bodies $K_1, \ldots, K_m \subset \mathbb{R}^d$ and $t_1, \ldots, t_m \geqslant 0$ are positive constants. A particularly important fact about mixed-volumes for the problem at hand is their behavior under averaged rotations [18]; specifically,

$$\begin{aligned} &\int_{SO(d)} V(K_1, \ldots, K_m, \boldsymbol{\omega} K_{m+1}, \ldots, \boldsymbol{\omega} K_d)\, \mathrm{d}\boldsymbol{\omega} \\ &\qquad = \frac{1}{\kappa_d} V(K_1, \ldots,_m, B_d[d-m]) V(B_d[m], K_{m+1}, \ldots, K_d), \end{aligned} \tag{16}$$

where $V(K[i], L[j])$ is a shorthand notation for the mixed volume $V(K, \ldots, K, L, \ldots, L)$ with $i$ copies of $K$ and $j$ copies of $L$.

The Aleksandrov–Fenchel inequality, which will be used later to prove a certain bound, states

$$V(K_1, K_2, K_3, \ldots, K_n)^2 \geqslant V(K_1, K_1, K_3, \ldots, K_n) V(K_2, K_2, K_3, \ldots, K_n). \tag{17}$$

For more details, see theorem 7.3.1 of [18].

## 3. General formula for the rotationally-averaged exclusion volume

### 3.1. Exclusion volume

We now have the tools needed to derive a formula for the exclusion volume for convex bodies with random orientations.

**Lemma 1.** *For any convex bodies $K, L \subset \mathbb{R}^d$, the rotationally-averaged exclusion volume is explicitly given in terms of the mixed volumes by the following formula:*

$$v_{\mathrm{ex}}(K, L) = \frac{1}{\kappa_d} \sum_{i=0}^{d} \binom{d}{i} W_i(L) W_{d-i}(K). \tag{18}$$



J. Stat. Mech. (2022) 093404

**Proof.** From the definition of the mixed volume in relation (15), we have

$$\mathrm{Vol}(K+\boldsymbol{\omega}L)=\sum_{i=0}^{d}\binom{d}{i}V(K[i],\boldsymbol{\omega}L[d-i]). \tag{19}$$

Thus, equations (16) and (19) give us the following:

$$\begin{aligned} v_{\mathrm{ex}}(K,L) &= \int_{SO(d)}\mathrm{Vol}(K+\boldsymbol{\omega}L)\,\mathrm{d}\boldsymbol{\omega} \\ &= \int_{SO(d)}\sum_{i=0}^{d}\binom{d}{i}V(K[i],\boldsymbol{\omega}L[d-i])\,\mathrm{d}\boldsymbol{\omega} \\ &= \sum_{i=0}^{d}\binom{d}{i}\left[\frac{1}{\kappa_d}V(K[i],B_d[d-i])V(B_d[i],L[d-i])\right] \\ &= \frac{1}{\kappa_d}\sum_{i=0}^{d}\binom{d}{i}W_{d-i}(K)W_i(L). \end{aligned} \tag{20}$$

This completes the proof.

**Remark.** Lemma 1 is actually a special case of the so-called *kinematic formula*, in which no assumption is made about the orientations of the bodies; see, for example, equation (30) in [19].

Of particular interest for us is the situation when we have two copies of the same body $K$, in which case the exclusion volume formula of lemma 1 simplifies as follows:

$$v_{\mathrm{ex}}(K)=v_{\mathrm{ex}}(K,K)=\frac{1}{\kappa_d}\sum_{i=0}^{d}\binom{d}{i}W_{d-i}(K)W_i(K). \tag{21}$$

### 3.2. Quermassinegrals as cross-sectional volumes

Schneider [18] introduces the *area measures* $S_m(K,\omega)$ for a convex body $K$, where $\omega$ a measurable set of rotations. As their name suggests, they give a measure of the $m$-dimensional cross-sectional volume of $K$ averaged over $\omega$. In [18], the quermassintegrals are introduced as

$$W_i(K)=\frac{1}{d}S_{d-i}(K,\mathbb{S}^{d-1}), \tag{22}$$

which is equivalent to the definition we have given. For example, if $K$ is a $d$-dimensional body in $\mathbb{R}^d$, then the area measure $S_{d-1}(K,\mathbb{S}^{d-1})$ is exactly equal to the surface area of $K$, which we denote by $s(K)$. More precisely, $S_{d-1}(K,\mathbb{S}^{d-1})$ is equal to the $(d-1)$-dimensional Hausdorff measure of the set $\bigcup_{u\in\mathbb{S}^{d-1}}F(K,u)$, where $F(K,u)$ is the intersection of $K$ with its supporting hyperplane with normal $u$. Thus, provided that $K$ is



J. Stat. Mech. (2022) 093404

sufficiently smooth (including polyhedra), we have

$$W_1(K) = \frac{s(K)}{d}. \tag{23}$$

Similarly, $W_{d-1}(K)$ is related to the *radius of mean curvature*, $\bar{R}(K)(K)$, via the notion of the *mean width*, denoted by $\bar{w}(K)$. Using the fact that $\bar{R}(K) = \bar{w}(K)/2$ [9], we have that

$$W_{d-1}(K) = \frac{\kappa_d}{2}\bar{w}(K) = \kappa_d \bar{R}(K). \tag{24}$$

Observe that directly from the definition of the mixed volume, $V(K, \ldots, K) = v(K)$ for any convex body $K$, so that the following two simple relationships immediately follow:

$$W_0(K) = v(K), \tag{25}$$

$$W_d(K) = \kappa_d. \tag{26}$$

Other quermassintegrals in terms of other cross-sectional volumes can be obtained from [18].

### 3.3. Comparison to the Torquato–Jiao exclusion-volume formula

Torquato and Jiao [9] proposed the following formula for the exclusion volume in $d$ dimensions:

$$v_{\mathrm{ex}}(K) \simeq 2v(K) + \frac{2^d - 2}{d} s(K)\bar{R}(K)(K), \tag{27}$$

where $s(K)$ is the surface area of $K$ and $\bar{R}(K)$ is the radius of mean curvature of $K$. We show here that formula (27) is exact for all bodies in dimensions 1, 2, and 3 and for greater dimensions only specific classes of bodies. Interestingly, we prove that for $d \geqslant 4$ formula (27) is generally a lower bound on the exact exclusion volume, given by relation (21) for $d \geqslant 4$.

First, we compare formulas (21) and (27), in the first three space dimensions. For $d = 1$, formula (21) together with (25) and (23) yields

$$v_{\mathrm{ex}}(K) = W_0(K)W_1(K) = 2v(K), \tag{28}$$

which agrees with formula (27). For $d = 2$, formula (21) together with (24)–(26) yields

$$\begin{aligned} v_{\mathrm{ex}}(K) &= \frac{1}{\kappa_2}(W_0(K)W_2(K) + 2W_1(K)^2 + W_0(K)W_2(K)) \\ &= \frac{1}{\pi}\left(2\pi v(K) + \frac{1}{2}s(K)^2\right) = 2v(K) + \frac{s(K)^2}{2\pi} \end{aligned} \tag{29}$$

which agrees with formula (27). For $d = 3$, formula (21) together with (23)–(26) yields



J. Stat. Mech. (2022) 093404

$$\begin{aligned} v_{\mathrm{ex}}(K) &= \frac{2}{\kappa_3}(W_0(K)W_3(K) + 3W_1(K)W_2(K)) \\ &= \frac{2}{\kappa_3}\left(\kappa_3 v(K) + 3\frac{s(K)}{3}(\kappa_3 \bar{R}(K))\right) \\ &= 2v(K) + 2s(K)\bar{R}(K). \end{aligned} \tag{30}$$

Thus, formula (27) agrees with formula (21) in dimensions 1, 2, and 3, since in these dimensions only the quermassintegrals $W_0$, $W_1$, $W_{d-1}$, and $W_d$ are relevant. In higher dimensions, however, the other quermassintegrals will generally play a role.

The Aleksandrov–Fenchel inequality (17) will allow us to continue our comparison of the formulas (21) and (27). Since the mixed volumes are symmetric [18], it follows that for the quermassintegrals, we have

$$W_i(K)^2 \geqslant W_{i-1}(K)W_{i+1}(K). \tag{31}$$

This inequality implies the inequality

$$W_i(K)/W_{i-1}(K) \geqslant W_{i+1}(K)/W_i(K) \tag{32}$$

and by iterating this we find that for any $j \geqslant i$ and sufficiently small $k$ (such that $i-k \geqslant 0$ and $j+k \leqslant d$) we have

$$W_i(K)W_j(K) \geqslant W_{i-1}W_{j+1}(K) \geqslant W_{i-k}(K)W_{j+k}(K), \tag{33}$$

where the second inequality follows from iterating the first. Thus, for all $i$,

$$W_i(K)W_{d-i}(K) \geqslant W_1(K)W_{d-1}(K). \tag{34}$$

Now we can write

$$\begin{aligned} v_{\mathrm{ex}}(K) &= \frac{1}{\kappa_d}\sum_{i=0}^{d}\binom{d}{i}W_{d-i}(K)W_i(K) \\ &= \frac{1}{\kappa_d}\left(2W_0(K)W_d(K) + \sum_{i=1}^{d-1}\binom{d}{i}W_i(K)W_{d-i}(K)\right) \\ &\geqslant \frac{1}{\kappa_d}\left(2W_0(K)W_d(K) + \sum_{i=1}^{d-1}\binom{d}{i}W_1(K)W_{d-1}(K)\right) \\ &= \frac{1}{\kappa_d}\left(2W_0(K)W_d(K) + (2^d-2)W_1(K)W_{d-1}(K)\right) \\ &= \frac{1}{\kappa_d}\left(2\kappa_{\mathrm{d}} v(K) + (2^d-2)\frac{s(K)}{d}\kappa_d\bar{R}(K)\right) \\ &= 2v(K) + \frac{2^d-2}{d}s(K)\bar{R}(K). \end{aligned} \tag{35}$$



J. Stat. Mech. (2022) 093404

In summary,

$$v_{\mathrm{ex}}(K) = \frac{1}{\kappa_d}\sum_{i=0}^{d}\binom{d}{i}W_{d-i}(K)W_i(K) \geqslant 2v(K) + \frac{2^d-2}{d}s(K)\bar{R}(K). \tag{36}$$

Thus, we have proven that the formula (27) is a rigorous lower bound on $v_{\mathrm{ex}}(K)$.

The fact that these two formulas are linked via such an elegant argument is rather surprising, and it leaves one wondering if there is a deeper reason. The method of the proof and the fact that the formulas agree in the first three space dimensions do, nonetheless, give an intuitive explanation: both formulas are derived from an average measure of a body's cross-sectional volumes. Formula (27) takes into account only one-, $(d-1)$-, and $d$-dimensional volumes, and hence does not account for information from other dimensional volumes, if they exist. Formula (21) does take these other contributions into account, and thus it generally produces a larger value for the exclusion volume for $d \geqslant 4$.

Are there situations under which the inequality in the bound (36) becomes an equality for $d \geqslant 4$? We now show that there is a class of bodies for which the two formulas do agree exactly. A sufficient condition to guarantee the bounds are equal is that $W_i(K)^2 = W_{i-1}(K)\,W_{i+1}(K)$ for $i \in \{2, \ldots, d-2\}$; then, we would have

$$W_i(K)/W_{i-1}(K) = W_{i+1}(K)/W_i(K) \tag{37}$$

for all $i$, and upon iterating this equality we find that

$$W_i(K)W_{d-i}(K) = W_1(K)W_{d-1}(K) \tag{38}$$

for all $i$. Then all of the inequalities in relation (35) become equalities, and the two formulas (21) and (27) agree exactly.

It is not known in general when $W_i(K)^2 = W_{i-1}(K)\,W_{i+1}(K)$; however, it is known that if $K$ is a $d$-dimensional centrally symmetric convex body then $W_i(K)^2 = W_{i-1}(K)\,W_{i+1}(K)$ if and only if $K$ is a $(d-i-1)$-tangential body to a sphere; see theorem 7.6.20 of [18]. If this holds for $i \in \{2, \ldots, d-2\}$, then this is equivalent to $K$ being a one-tangential body to a sphere, which is also called a *cap body* [18]. A cap body is the convex hull of a sphere and a countable sequence of points $\{x_n\}$ such that for distinct $x_i$ and $x_j$, the line going through $x_i$ and $x_j$ intersects the sphere.

## 4. Determination of quermassintegrals for specific convex bodies in $\mathbb{R}^d$

With the relation (21), the problem of determining the rotationally-averaged exclusion volume for specific convex bodies reduces to the problem of obtaining formulas for the corresponding quermassintegrals $W_0(K), \ldots, W_d(K)$. We obtain such formulas in arbitrary dimension for the following convex bodies: sphere, cube, right parallelpiped, convex cylinder, spherocylinder, general ellipsoid, ellipsoid of revolution, regular simplex, and cross-polytope as well as lower-dimensional bodies, such as the line segment, spherical hyperplate and cubical hyperplate. It bears repeating that the cube, regular simplex



J. Stat. Mech. (2022) 093404

and cross-polytope are the only regular polytopes possible for $d \geqslant 5$ [20]. For some of the convex bodies, we also provide explicit formulas for the exclusion volume $v_{\mathrm{ex}}(K)$ via (21) that applies in arbitrary dimensions. In the remaining cases, while closed-form analytical formulas for $v_{\mathrm{ex}}(K)$ can be presented, we do not do so because the resulting equations would be cumbersomely long.

Throughout the following discussion, $i \in \{0, \ldots, d\}$ denotes the index of the quermassintegral. As the input to the quermassintegrals is obvious, we write $W_i$ instead of $W_i(K)$. We denote the surface area of the unit sphere $B_d$ in $\mathbb{R}^i$ as

$$\beta_i = \mathrm{d}\kappa_i \tag{39}$$

where

$$\kappa_i = \frac{\pi^{i/2}}{\Gamma(1 + i/2)} \tag{40}$$

is the corresponding volume of the unit sphere, as obtained from (14).

### 4.1. Spheres

For a sphere (ball) of radius $a$, we have the following simple formula for the quermassintegrals [16]:

$$W_i = \kappa_d a^{d-i}. \tag{41}$$

Using the identity $\sum_{i=0}^{d} \binom{d}{i} = 2^d$, formula (21) and the fact $\kappa_d$ does not depend on the index $i$, immediately leads to the well-known result that for spheres,

$$\frac{v_{\mathrm{ex}}(K)}{v(K)} = 2^d. \tag{42}$$

### 4.2. Cube

For a cube with side length $b$, we have the following simple formula [16]:

$$W_i = \kappa_i b^{d-i}. \tag{43}$$

Hence, according to formula (21), we have that the explicit formula for the dimensionless exclusion volume for cubes is given by

$$\frac{v_{\mathrm{ex}}(K)}{v(K)} = \frac{1}{\kappa_d} \sum_{i=0}^{d} \binom{d}{i} \kappa_i \kappa_{d-i}. \tag{44}$$

For example, for $d = 3, 4, 5$ and 6, we obtain from (44) the exact results $v_{\mathrm{ex}}(K)/v(K) = 11, 25.5812218\ldots, 70.75$ and $184.3523083\ldots$, respectively.

Elementary analysis of formula (44) in the high-$d$ limit leads to the following asymptotic formula for the dimensionless exclusion volume for the cube:



J. Stat. Mech. (2022) 093404

$$\frac{v_{\mathrm{ex}}(K)}{v(K)} \sim \frac{2^{3(d+1)/2}}{\sqrt{3\pi d}} \quad (d \to +\infty). \tag{45}$$

Comparing formulas (42) and (45), we see that the dimensionless exclusion volume for cubes relative to that for spheres grows exponentially faster according to $2^{d/2}/\sqrt{d}$ as $d$ becomes large. We note that this asymptotic formula already leads to very accurate predictions of $v_{\mathrm{ex}}(K)/v(K)$ for cubes even in relatively low dimensions, say $d \geqslant 6$, as can be seen from the results presented in section 6. In addition, randomly oriented hypercubes have a much larger dimensionless exclusion volume than oriented hypercubes.

### 4.3. Right parallelepiped

A right parallelpiped with edge lengths $b_k$, $k = \{1, \ldots, d\}$ is defined to be the product $[0, b_1] \times \cdots \times [0, b_d]$. To write the formula for its quermassintegrals, let $\sigma_k$ denote the $k$th elementary symmetric polynomial on $d$ variables, namely

$$\sigma_k(x_1, \ldots, x_d) = \sum_{1 \leqslant i_1 \leqslant \ldots \leqslant i_k \leqslant d} x_{i_1} \ldots x_{i_k}. \tag{46}$$

Then we have the following expressions for $W_i(K)$ [16]:

$$W_i = \frac{\kappa_i}{\binom{d}{i}} \sigma_{d-i}(b_1, \ldots, b_d). \tag{47}$$

According to formula (21), we have the explicit formula for the dimensionless exclusion volume, which is given by

$$\frac{v_{\mathrm{ex}}(K)}{v(K)} = \frac{1}{\kappa_d \Pi_{k=1}^d b_k} \sum_{i=0}^{d} \frac{\kappa_i \kappa_{d-i}}{\binom{d}{d-i}} \sigma_i \sigma_{d-i} \tag{48}$$

where $\sigma_k$ is given by equation (46).

### 4.4. Right parallelepiped with a specific aspect ratio

In applications, one may often encounter right parallelpipeds $[0, b_1] \times \cdots \times [0, b_d]$ where all $b_k$ are equal ($b_k = b$) except for one, say $b_1 = h$. We call such a body a right parallelepiped with an aspect ratio $\gamma$, defined as $\gamma = h/b$. We then have the following formula for the quermassintegrals which is more efficient to calculate in simulations:

$$W_i = \frac{\kappa_i}{\binom{d}{i}} \left[ \binom{d-1}{d-i} b^{d-i} + \left( \binom{d}{d-i} - \binom{d-1}{d-i} \right) \gamma b^{d-i} \right]. \tag{49}$$

### 4.5. Convex cylinder

A convex cylinder in $\mathbb{R}^d$ is the Cartesian product of a $(d-1)$-dimensional sphere and an interval. More specifically, let $B$ be a $(d-1)$-dimensional sphere of radius $a$ in $\mathbb{R}^{d-1}$.



J. Stat. Mech. (2022) 093404

Then let $C = (B \times \{0\}) \times [0, h]$. The body $C$ is called a convex cylinder with radius $a$ and height $h$, and we have the following formulas [16]:

$$W_i = \frac{\kappa_{d-1}}{d}\left(\frac{\beta_{i-1}}{\kappa_{i-1}}a^{d-i} + (d-i)a^{d-i-1}h\right) \quad i \geqslant 2, \tag{50}$$

and

$$W_0 = \kappa_{d-1}a^{d-1}h, \qquad W_1 = \frac{\kappa_{d-1}}{d}(2a^{d-1} + (d-1)a^{d-2}h). \tag{51}$$

### 4.6. Spherocylinder

A spherocylinder is the Minkowski sum of a sphere and a line segment, and thus a spherocylinder is an $\varepsilon$-neighborhood of a line segment. Equation (13.27) of [16] gives a formula for the quermassintegrals of an $\varepsilon$-neighborhood of a body $K$, as follows:

$$W_i(K + \varepsilon B_d) = \sum_{j=0}^{d-i}\binom{d-i}{j} jW_{i+j}(K)\varepsilon^j. \tag{52}$$

When $K$ is a line segment of length $h$ and when $\varepsilon = a$, this reduces to the following formula for a spherocylinder of height $h$ and radius $a$:

$$W_i = a^{d-i}\kappa_d + (d-i)a^{d-i-1}\frac{\kappa_{d-1}}{d}h. \tag{53}$$

High-$d$ asymptotic analysis of the exclusion-volume formula (21) together with (53) leads to the following exact scaling behavior for the dimensionless exclusion volume of a spherocylinder with $h > 0$ and finite:

$$\frac{v_{\mathrm{ex}}(K)}{v(K)} \sim \frac{2^d\sqrt{d}}{\sqrt{32\pi}}\frac{h}{a} + \frac{2^d 3}{4}. \tag{54}$$

We see that for positive, finite values of $h$, the dimensionless exclusion volume for a spherocylinder relative to that of a sphere only rises like the square root of the dimension.

### 4.7. General ellipsoid

An ellipsoid with axes $a_k$, $k = \{1, \ldots, d\}$ is the image of a sphere with radius 1 under the linear transformation $(x_1, \ldots, x_d) \to (a_1x_1, \ldots, a_{\mathrm{d}}x_d)$. Let $\{v_j\}_{j=1}^i$ be independent centered non-degenerate Gaussian random vectors in $\mathbb{R}^d$ whose $k$th coordinates are distributed

$$v_j^{(k)} \sim N(0, a_k^2). \tag{55}$$

Let $M$ be a $i \times d$ matrix whose $j$th row is $v_j$, in other words $M = (v_1, \ldots, v_i)^{\mathrm{T}}$. Then we have the following [26]:

$$W_i = \frac{\kappa_i}{\binom{d}{d-i}}\frac{(2\pi)^{d-i}}{(d-i)!}\mathbb{E}\left(\sqrt{\det(MM^{\mathrm{T}})}\right), \tag{56}$$



J. Stat. Mech. (2022) 093404

where $\mathbb{E}(\cdot)$ denotes the expectation function. While this formula cannot be calculated exactly in general, the expectation can be readily calculated to arbitrary accuracy.

### 4.8. Ellipsoid of revolution

An ellipsoid of revolution in $\mathbb{R}^d$ is an ellipsoid with axes $a_1, \ldots, a_d$ where every $a_k$ except for $a_1$ has the same value. Furthermore, we assume by convention that $a_1 < a_k$ for $k \neq 1$. We let the common length be denoted by $a$ and define $\lambda$ so that $a_1 = \lambda a$.

Now let $F$ denote the hypergeometric function, namely

$$F(a, b, c\,; z) = \sum_{n=0}^{\infty} \frac{(a)_n (b)_n}{(c)_n} \frac{z^n}{n!}, \tag{57}$$

where $(x)_n$ is the Pochhammer symbol, defined as

$$(x)_n = \frac{\Gamma(x+n)}{\Gamma(x)} = x(x+1)\ldots(x+n-1). \tag{58}$$

Then we have the following [16]:

$$W_i = \kappa_d \lambda^{i+1} a^{d-i} F\left(\frac{d+1}{2}, \frac{i}{2}, \frac{d}{2}\,; 1-\lambda^2\right). \tag{59}$$

### 4.9. Regular simplex

A simplex in $\mathbb{R}^d$ is the convex hull of $d+1$ points. A regular simplex is a simplex whose edges all have equal length. For a regular simplex with edge length $c$, we have [27]:

$$W_0 = \left(\frac{c}{\sqrt{2}}\right)^d \frac{\sqrt{d+1}}{d!}, \quad W_d = \kappa_d \tag{60}$$

For $1 \leqslant i < d$,

$$W_i = \left(\frac{c}{\sqrt{2}}\right)^{d-i} \frac{\kappa_i}{\binom{d}{d-i}} \binom{d+1}{d-i+1} \frac{\sqrt{d-i+1}}{d!} \gamma(T_{d-i}, T_d) \tag{61}$$

where $\gamma(T_{d-i}, T_d)$ is the external angle of the simplex at a $(d-1)$-dimensional face, calculated by

$$\gamma(T_{d-i}, T_d) = \sqrt{\frac{d-i+1}{\pi}} \int_{-\infty}^{\infty} e^{-(d-i+1)x^2} \left(\frac{1}{\sqrt{\pi}} \int_{-\infty}^{x} e^{-y^2}\, \mathrm{d}y\right)^i \mathrm{d}x \tag{62}$$

### 4.10. Cross-polytope

The canonical cross-polytope is the convex hull of the $2d$ unit vectors $e_1, -e_1, \ldots, e_d, -e_d$. We recall that a two-dimensional cross-polytope is a square, a three-dimensional cross-polytope is a regular octahedron, and a four-dimensional cross-polytope is a 16-cell.



J. Stat. Mech. (2022) 093404

The facets of a cross-polytope for $d \geqslant 3$ are regular simplices in dimension $d-1$. For a regular cross-polytope of side length $c$ we have [27]:

$$W_0 = \frac{(c\sqrt{2})^d}{d!}, \qquad W_d = \kappa_d. \tag{63}$$

For $1 \leqslant i < d$,

$$W_i = \left(\frac{c}{\sqrt{2}}\right)^{d-i} 2^{d-i+1} \frac{\kappa_i}{\binom{d}{d-i}} \binom{d}{k+1} \frac{\sqrt{d-i+1}}{d!} \gamma(T_{d-i}, C_d^{\Delta}) \tag{64}$$

where again $\gamma(T_{d-i}, C_d^{\Delta})$ denotes the external angle of the cross-polytope at a $T_{d-i}$ face, calculated by

$$\gamma(T_{d-i}, C_d^{\Delta}) = \sqrt{\frac{k+1}{\pi}} \int_0^{\infty} e^{-(d-i+1)x^2} \left(\frac{2}{\sqrt{\pi}} \int_0^x e^{-y^2}\, \mathrm{d}y\right)^{i-1} \mathrm{d}x. \tag{65}$$

### 4.11. Spherical hyperplates

The derivation of these formulas is given in appendix A. For a spherical hyperplate of radius $a$, we have for $i = 0$ and $i = 1$

$$W_0 = 0, \qquad W_1 = \frac{2\kappa_{d-1}}{d} a^{d-1} \tag{66}$$

and for $i \geqslant 2$

$$W_i = \left(\frac{\kappa_{d-1}}{\kappa_{i-1}} \cdot \frac{i}{d}\right) \kappa_i a^{d-i}. \tag{67}$$

According to equation (21), the explicit formula for the exclusion volume of spherical hyperplates is given by

$$\frac{v_{\mathrm{ex}}(K_{\mathrm{H}})}{v_{\mathrm{eff}}(K_{\mathrm{H}})} = \frac{\Gamma(d/2+1)}{\pi^{d/2}} \left[\frac{2\kappa_{d-1}^3}{\kappa_d \kappa_{d-2}} \frac{(d-1)}{d^2} + \frac{1}{\kappa_d} \sum_{i=1}^{d-1} \binom{d}{i} \frac{\kappa_i \kappa_{d-i} \kappa_{d-1}^2}{\kappa_{i-1} \kappa_{d-i-1}} \frac{(d-i)}{d^2}\right], \tag{68}$$

where $v_{\mathrm{eff}}(K_{\mathrm{H}})$ is the effective volume given in equation (6), which is the volume of a $d$-dimensional sphere with radius $r = a$. It is clear that $v_{\mathrm{eff}}(K_{\mathrm{H}})$ for a spherical hyperplate must have the same high-$d$ scaling as a full-dimensional sphere in $d$ dimensions, i.e. it must scale as $2^d$.

### 4.12. Cubical hyperplates

As for spherical hyperplates, the derivation of the following formulas is given in appendix A. For a cubical hyperplate of edge length $b$, we have for $i = 0$

$$W_0 = 0 \tag{69}$$



J. Stat. Mech. (2022) 093404

and for $i \geqslant 1$

$$W_i = \left(\frac{i}{d}\right)\kappa_i b^{d-i}. \tag{70}$$

According to equation (21), the explicit formula for the exclusion volume of cubical hyperplates is given by

$$\frac{v_{\mathrm{ex}}(K_{\mathrm{H}})}{v_{\mathrm{eff}}(K_{\mathrm{H}})} = \frac{\Gamma(d/2+1)}{\Gamma((d+1)/2)^{\frac{d}{d-1}}}\frac{1}{\kappa_d}\sum_{i=1}^{d-1}\binom{d}{i}\frac{(d-i)i}{d^2}\kappa_i\kappa_{d-i}, \tag{71}$$

where the effective volume $v_{\mathrm{eff}}(K_{\mathrm{H}})$ of a $d$-dimensional sphere, defined by equation (6), has radius $r = \Gamma((d+1)/2)^{1/(d-1)}b/\pi^{1/2}$. This radius corresponds to the $(d-1)$-dimensional cubical hyperplate having the same volume as the $(d-1)$-dimensional spherical hyperplate. Similar to the case of cubes, our analysis of formula (71) in the high-$d$ limit leads to the following asymptotic formula:

$$\frac{v_{\mathrm{ex}}(K_{\mathrm{H}})}{v(K_{\mathrm{H}})} \sim \frac{\sqrt{e}}{4}\frac{2^{3(d+1)/2}}{\sqrt{3\pi d}} \qquad (d \to +\infty). \tag{72}$$

It can be seen that the cubical hyperplates possess the same large-$d$ asymptotic scaling as cubes (cf equation (45)), up to a constant. Comparing formulas (42) and (72), we see that the dimensionless exclusion volume for cubical hyperplates relative to that for spheres grows exponentially as $2^{d/2}/\sqrt{d}$ for large $d$.

### 4.13. Line segment

Except for $W_{d-1}$ and $W_d$, all of the quermassintegrals of a line segment in $\mathbb{R}^d$ are exactly 0. This is because a line segment is intrinsically one-dimensional, and so it can only have zero- and one-dimensional cross-sectional volumes. The issue of the quermassintegrals of low-dimensional bodies is discussed in more detail and generality in appendix A. For the line segment of length $\ell$ in $\mathbb{R}^d$, we have the following formulas [16]: for $d \geqslant 2$,

$$W_i = 0 \quad (i = 0, 1, \ldots, d-2), \qquad W_{d-1} = \frac{\kappa_{d-1}}{d}\ell, \qquad W_d = \kappa_d. \tag{73}$$

For $d = 1$,

$$W_0 = \ell, \qquad W_1 = 2, \tag{74}$$

which is identical to the case of overlapping rods of length $\ell$. The relations above together with formula (21) prove that the exclusion volume for a line segment in $\mathbb{R}^d$ vanishes for $d \geqslant 3$.



J. Stat. Mech. (2022) 093404

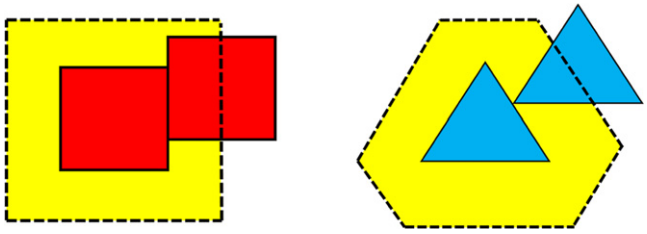


**Figure 3.** Illustration of the exclusion volume of two-dimensional convex bodies, each with the same orientation. In each of the two examples, the exclusion volume is the region interior to the boundary delineated by the dashed lines. (Left) Centrally symmetric spherocylinder. (Right) Non-centrally symmetric triangle.

## 5. Extremal values for exclusion volumes of oriented and non-oriented bodies

### 5.1. Oriented exclusion volume

The estimates (4) and (5) apply to systems of hyperparticles with any orientation distribution. For a system of uniformly oriented hyperparticles (figure 3), there are exact results for the dimensionless quantity $v_{\rm ex}(K)/v(K)$ of (4) worth discussing here.

A result known as the Roger–Shepherd inequality (theorem 10.1.4 of [18]) states that for any full-dimensional convex body $K \subset \mathbb{R}^d$ (i.e. a convex body with nonzero volume), we have

$$2^d \leqslant \frac{v(K-K)}{v(K)} \leqslant \binom{2d}{d}. \tag{75}$$

The quantity $v(K-K)$ resembles the quantity $v(K-\boldsymbol{\omega}K)$ appearing in the definition of the exclusion volume, as specified by relation (12).

If we assume that we are working in a system where all particles have an identical, fixed orientation, then it is reasonable to define an 'oriented' exclusion volume in the same way that we defined the exclusion volume for randomly oriented particles, but without the step of averaging over orientations. Following (1), let $K$ be a convex body with some orientation $\boldsymbol{\omega}$. Then $f(\mathbf{r},\boldsymbol{\omega}\,;\ K)$ is the indicator function of the exclusion zone of $K$ with respect to a copy of $K$ centered at $\mathbf{r}$ with orientation $\boldsymbol{\omega}$. Then the *oriented exclusion volume* of $K$, which we denote $v_{\rm ex}^o$ for clarity, is given by

$$\begin{aligned} v_{\rm ex}^o(K) &= \int_{\mathbb{R}^d} f(\mathbf{r},\boldsymbol{\omega}\,;K)\,{\rm d}\mathbf{r} \\ &= {\rm Vol}((K,K)) \\ &= v(K-K), \end{aligned} \tag{76}$$

where we have used (11) and the fact that $Z(K,K) = K-K$. The randomly oriented non-spherical hyperparticles generally have a much higher dimensionless exclusion volume than the oriented ones.



J. Stat. Mech. (2022) 093404

### 5.2. Extremal exclusion volumes for oriented hyperparticles

Combining the definition (76) and the Roger–Shepherd inequality (75), we derive the following inequality for any convex, full dimensional, oriented hyperparticle $K$:

$$2^d \leqslant \frac{v_{\mathrm{ex}}^o(K)}{v(K)} \leqslant \binom{2d}{d}. \tag{77}$$

It is known that equality holds on the left in formula (77) precisely when $K$ is centrally symmetric, and that equality holds on the right precisely when $K$ is a simplex (see theorem 10.1.4 of [18]). Thus, when restricted to oriented particles, we have the fairly strong result that $v_{\mathrm{ex}}^o(K)/v(K)$ is *minimized* for centrally symmetric particles and *maximized* for simplices, which has the high-$d$ asymptotic behavior of $2^{2d}/d^{3/2}$. This means that the ratio of $v_{\mathrm{ex}}^o(K)/v(K)$ for simplices relative to that for spheres and other centrally symmetric bodies grows like $2^d/d^{3/2}$.

### 5.3. Extremal exclusion volumes for non-oriented hyperparticles

For non-oriented hyperparticles, a result of the same strength as in (77) is not known for $v_{\mathrm{ex}}(K)/v(K)$. For randomly oriented particles, however, we can recover the lower-bound side of the inequality (77).

The Brunn–Minkowski inequality (theorem 7.1.1 of [18]) states that for two full dimensional convex bodes $K$ and $L$ in $\mathbb{R}^d$, we have

$$v(K+L)^{1/d} \geqslant v(K)^{1/d} + v(L)^{1/d}. \tag{78}$$

Thus, for any rotation $\boldsymbol{\omega}$ we have

$$\begin{aligned} v(K+\boldsymbol{\omega}K)^{1/d} &= v(K+\boldsymbol{\omega}K)^{1/d} \\ &\geqslant v(K)^{1/d} + v(\boldsymbol{\omega}K)^{1/d} \\ &= v(K)^{1/d} + v(K)^{1/d} \\ &= 2v(K)^{1/d} \end{aligned} \tag{79}$$

so that

$$v(K+\boldsymbol{\omega}K) \geqslant 2^d v(K). \tag{80}$$

From the definition of the randomly oriented exclusion volume (12), we then have

$$v_{\mathrm{ex}}(K) = \int_{SO(d)} v(K+\boldsymbol{\omega}K)\,\mathrm{d}\boldsymbol{\omega} \geqslant \int_{SO(d)} 2^d v(K)\,\mathrm{d}\boldsymbol{\omega} = 2^d v(K) \tag{81}$$

and we thus derive

$$\frac{v_{\mathrm{ex}}(K)}{v(K)} \geqslant 2^d. \tag{82}$$

Here, we recover the same lower bound as in the inequality (77), but for randomly oriented hyperparticles.



J. Stat. Mech. (2022) 093404

For (77), which applies to oriented bodies, we know that the equality on the left holds *exactly* when the body is centrally symmetric. This is not the case for randomly oriented particles, with a simple counterexample being the cube. However, it is at least true for spheres (balls), i.e. the lower bound is realizable by spheres. If $B_d$ denotes the unit sphere in $\mathbb{R}^d$, then $\boldsymbol{\omega} B_d = B_d$ for any rotation $\boldsymbol{\omega}$. Thus,

$$v(B_d + \boldsymbol{\omega} B_d) = v(B_d + B_d) = 2^d v(B_d) \tag{83}$$

and so

$$v_{\mathrm{ex}}(B_d) = \int_{SO(d)} v(B_d + \boldsymbol{\omega} B_d)\, \mathrm{d}\boldsymbol{\omega} = \int_{SO(d)} 2^d v(B_d)\, \mathrm{d}\boldsymbol{\omega} = 2^d v(B_d). \tag{84}$$

We then conclude that

$$\frac{v_{\mathrm{ex}}(B_d)}{v(B_d)} = 2^d. \tag{85}$$

In summary, from equations (82) and (85), we have, for full dimensional randomly oriented hyperparticles, the lower bound is realized for spheres, i.e.

$$\frac{v_{\mathrm{ex}}(K)}{v(K)} \geqslant 2^d = \frac{v_{\mathrm{ex}}(B_d)}{v(B_d)}. \tag{86}$$

## 6. Results

In this section, we employ the general formula (21) and the formulas for the quermassintegrals presented in section 4 to explicitly calculate the rotationally-averaged dimensionless exclusion volume $v_{\mathrm{ex}}(K)/v(K)$ for a variety of selected convex bodies, including the sphere, spherocylinder, cylinder, cube, parallelpiped, cross-polytope, simplex, as well as spherical and cubical hyperplates in dimensions $d = 2$ through 12. To the best of our knowledge, we report exact results for the exclusion volumes for these shapes for $d \geqslant 4$ for the first time. Our calculations for the first six dimensions for spheroids indicate that they are very similar to other elongated bodies across dimensions and the effects of elongation (i.e. aspect ratios) are illustrated using spherocylinders. Thus, we do not plot our results for spheroids and general ellipsoids. The calculations for general ellipsoids are highly non-trivial for $d \geqslant 4$, since their quermassintegrals involve statistical expectations. We subsequently use the new results on $v_{\mathrm{ex}}(K)/v(K)$ to obtain the second virial coefficient $B_2(K)$ for the these convex bodies in dimensions 2 through 12 using equation (3), as well as the estimates of the percolation threshold $\eta_{\mathrm{c}}$ across these dimensions using scaling relation (5).

### 6.1. Dimensionless exclusion volumes across dimensions

Figure 4 shows the dimensionless exclusion volume $v_{\mathrm{ex}}(K)/v(K)$ for the sphere, cube, spherocylinder with aspect ratio $h/a = 2$, cylinder with aspect ratio $h/a = 2$, parallelpiped with aspect ratio $h/b = 2$, cross-polytope, and simplex in dimensions



J. Stat. Mech. (2022) 093404

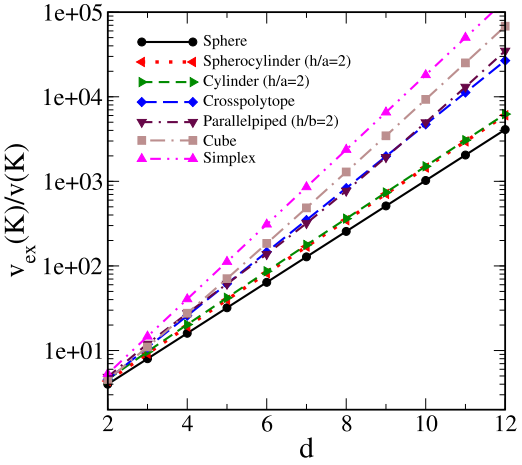



**Figure 4.** Rotationally-averaged dimensionless exclusion volume $v_{\rm ex}(K)/v(K)$ of a convex body $K$ for selected shapes, including the sphere, spherocylinder, cylinder, cube, parallelpiped, cross-polytope, and simplex in dimensions $d = 2$ to 12. The aspect ratios of the spherocylinder, cylinder and parallelpiped are taken to be relatively small so that all of the bodies considered are relatively compact.

$d = 2$ to 12. The values of $v_{\rm ex}(K)/v(K)$ for these shapes are provided in table A1 in the appendix. Our results for $d \geqslant 4$ appear to be new and supplement well-known results for these convex bodies in two and three dimensions [1]. We see from the figure that the sphere minimizes the ratio $v_{\rm ex}(K)/v(K)$ among the convex bodies examined. Of course, this is consistent with the rigorously exact relation (86) that the sphere minimizes $v_{\rm ex}(K)/v(K)$ among all convex bodies. On the other hand, simplices possess the largest ratio $v_{\rm ex}/v$ in any dimension among the compact shapes considered here. The cube possesses the next largest ratio $v_{\rm ex}(K)/v(K)$ among the bodies considered in figure 4. Interestingly, a least-squares fit of the data, whether in the range $6 \leqslant d \leqslant 12$ or $10 \leqslant d \leqslant 12$ yields a robust scaling behavior. In particular, for $10 \leqslant d \leqslant 12$, we find $v_{\rm ex}(K)/v(K) \sim 2^{1.44011\ldots d}$, which is close to the exact high-$d$ asymptotic scaling (45), which is controlled by the power law $2^{3d/2}$. Similarly, a least-squares fit of the data in figure 4 for simplices yields an approximate large-$d$ scaling behavior of $2^{1.6618\ldots d}$, which will be compared below to the corresponding high-$d$ scaling behavior for oriented simplices.

Not surprisingly, the spherocylinder and cylinder with the same aspect ratio (i.e. $h/a = 2$) possess very similar dimensionless exclusion volumes. The spherical caps of spherocylinders lead to a slightly smaller ratio $v_{\rm ex}(K)/v(K)$ compared to cylinders. The cross-polytope possesses a smaller $v_{\rm ex}/v$ than the cube in any dimension, and the difference increases as $d$ increases due to the former becoming more 'isotropic' (i.e. sphere-like) in shape in higher dimensions than cubes. The parallelpiped studied here possesses a cubical base with edge length $b$ and height $h$, with an aspect ratio $h/b = 2$. These parallelpipeds possess a larger ratio $v_{\rm ex}(K)/v(K)$ than the cube in lower dimensions ($d = 2, 3$), which then becomes smaller than that of the cubes for $d \geqslant 4$. A randomly oriented parallelpiped can make contact with another parallelpiped via either the cubical bases or the 'rectangular' facets. When contacting via the cubical bases, the centroids of the particles are further separated compared to contacts associated with the 'rectangular'



J. Stat. Mech. (2022) 093404

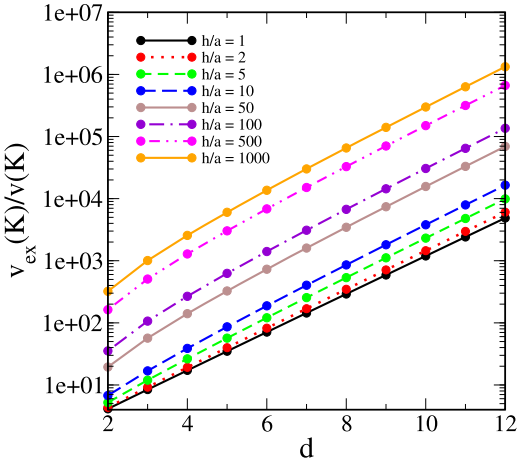



**Figure 5.** Rotationally-averaged dimensionless exclusion volume $v_{\rm ex}(K)/v(K)$ for spherocylinders at selected aspect ratios $h/a \in [1, 1000]$ in dimensions $d = 2$ to 12.

facets, which leads to a larger exclusion volume. In higher dimensions, the number of the 'rectangular' facets is much larger than that of the cubical bases. Therefore, the contribution of the 'base' contacts to the exclusion volume diminishes compared to the 'facet' contacts, leading to an orientation-averaged exclusion volume mainly dominated by centroid separations associated with length scale $b$ (i.e. the edge length of the cubical base). On the other hand, a larger height $h$ leads to a larger volume $v(K)$, and thus an overall smaller dimensionless exclusion volume.

To understand the effect of 'elongation' along an axis of symmetry of an anisotropic convex body with inequivalent axes on the dimensionless exclusion volume, we plot in figure 5 the ratio $v_{\rm ex}(K)/v(K)$ for spherocylinders for selected aspect ratios $h/a$ in the interval $[1, 1000]$ in dimensions $d = 2$ to 12 and list these values in table A2 in the appendix. For fixed $d$, $v_{\rm ex}/v$ increases significantly as the aspect ratio $h/a$ increases, as expected. Already for the relatively low dimensions in the range $d = 6$ to $d = 12$, $v_{\rm ex}(K)/v(K)$ has a scaling behavior with $d$ that is very close the exact high-$d$ asymptotic scaling (54), i.e. it is controlled by the power law $2^d$. By comparing these results for spherocylinders to the cases of simplices in figure 4, it is seen that if the aspect ratio $h/a$ is sufficiently large at fixed $d$, the ratio $v_{\rm ex}(K)/v(K)$ for spherocylinders can exceed that for simplices. Using the exact asymptotic formula (54) and the numerically fitted scaling of $2^{1.6618\ldots d}$ for simplices stated above, we find that, for fixed aspect ratio $h/a$, the crossover dimension $d^*$ scales like $\ln(h/a)$, i.e. for $d \lesssim d^*$, $v_{\rm ex}(K)/v(K)$ is largest for spherocylinders and for $d \gtrsim d^*$, $v_{\rm ex}(K)/v(K)$ is largest for simplices.

To get a sense of the behavior $v_{\rm ex}(K_{\rm H})/v_{\rm eff}(K_{\rm H})$ for lower-dimensional bodies of zero volume, we show the dimensionless exclusion volume for spherical and cubical hyperplates in dimensions $d = 3$ to 12 in figure 6. The values of their dimensionless exclusion volumes are given in table A3 in the appendix. It can be seen that spherical hyperplates possess a smaller value of $v_{\rm ex}(K_{\rm H})/v_{\rm eff}(K_{\rm H})$ than that of the cubical hyperplates, consistent with the trend for $d$-dimensional spheres and $d$-dimensional cubes. Specifically, our numerical scaling analysis of the data in figure 6 indicates that

J. Stat. Mech. (2022) 093404

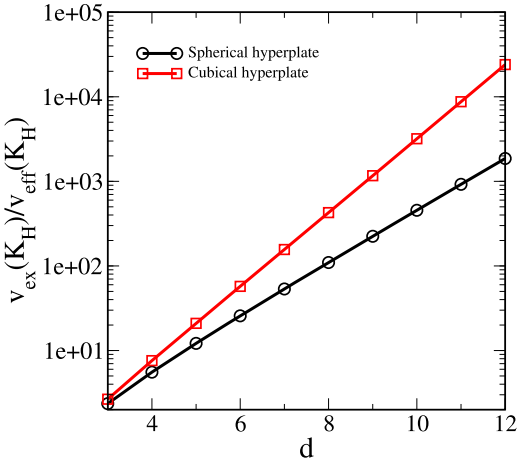



**Figure 6.** Rotationally-averaged dimensionless exclusion volume $v_{\rm ex}(K_{\rm H})/v_{\rm eff}(K_{\rm H})$ for spherical and cubical hyperplates in dimensions $d = 3$ to 12, where $v_{\rm eff}(K_{\rm H})$ is defined by (6).

$v_{\rm ex}(K_{\rm H})/v_{\rm eff}(K_{\rm H}) \sim 2^{1.01446\ldots d}$ for spherical hyperplates and $v_{\rm ex}(K_{\rm H})/v(K_{\rm H}) \sim 2^{1.45687\ldots d}$ for cubical hyperplates, the latter of which is consistent with the exact asymptotic formula (72). These results in relatively low dimensions are consistent with the exact result that $v_{\rm ex}(K_{\rm H})/v_{\rm eff}(K_{\rm H})$ for cubical hyperplates relative to that for spherical hyperplates must grow like $2^{d/2}$ for large $d$ (see section 4). We note that it is not meaningful to compare the dimensionless exclusion volumes for zero-volume $(d-1)$-dimensional hyperplates to those of nonzero-volume $d$-dimensional convex bodies, especially since the choice of the effective volume $v_{\rm eff}(K_{\rm H})$ used to make the exclusion volume for hyperplates dimensionless is arbitrary.

Finally, the dimensionless exclusion volume $v_{\rm ex}^0(K)/v(K)$ for oriented simplices in dimensions $d = 3$ to 12 in figure 7 and tabulated table A4 in the appendix. The figure compares results for simplices to those for spheres (or any other centrally symmetric convex body), which rigorously achieves the minimal value of $v_{\rm ex}^0(K)/v(K) = 2^d$ (cf section 5.1). Recall that for oriented simplices, the large-$d$ scaling behavior of $v_{\rm ex}^0(K)/v(K)$ is exactly given by $2^{2d}/d^{3/2}$ (cf section 5.1), which grows faster than that of spheres according to a factor of $2^d/d^{3/2}$ for large $d$. These substantially different growth rates of $v_{\rm ex}^0(K)/v(K)$ for simplices and spheres is evident in figure 7. In addition, the large-$d$ scaling for oriented simplices is exponentially larger than that of randomly oriented simplices, which we found earlier to be $2^{1.6618\ldots d}$.

### 6.2. Dimensionless second virial coefficients across dimensions

Figures 8 and 9 show the dimensionless second virial coefficients $B_2(K)/v(K)$ for selected convex bodies and spherocylinders with different aspect ratios across dimensions, respectively. Since $B_2(K)$ is trivially related to $v_{\rm ex}(K)$ via equation (3), the behaviors of $B_2(K)/v(K)$ across dimensions follow exactly those for the dimensionless exclusion vol-



J. Stat. Mech. (2022) 093404

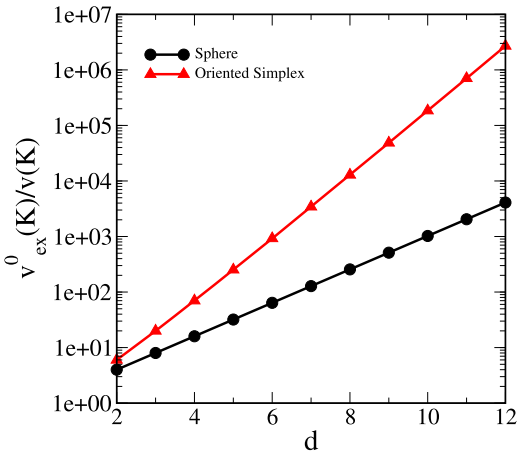



**Figure 7.** Dimensionless exclusion volume $v^0_{\rm ex}(K)/v(K)$ for oriented simplices in dimensions $d = 2$ to 12, compared to that of spheres.

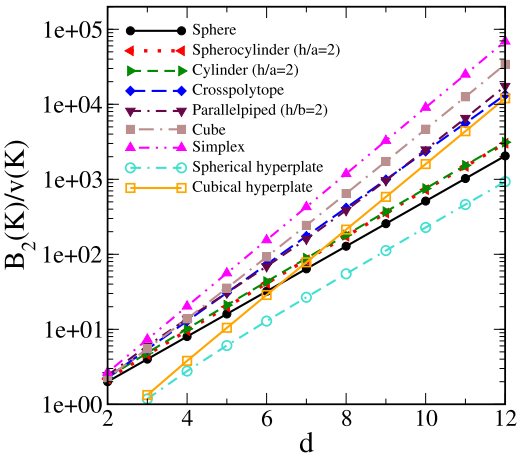



**Figure 8.** Dimensionless second virial coefficient $B_2(K)/v(K)$ for randomly oriented convex bodies for selected shapes, including the sphere, spherocylinder, cylinder, cube, parallelpiped, cross-polytope, and simplex in dimensions $d = 2$ to 12, as well as spherical and cubical hyperplates in dimensions $d = 3$ to 12.

ume $v_{\rm ex}(K)/v(K)$ discussed in the previous subsection. While $B_2(K)$ has long been known for these convex bodies in two and three dimensions [1], our results for $d \geqslant 4$ appear to be new. It is useful to reiterate that among the shapes considered, the sphere minimizes $B_2(K)/v(K)$ in any $d$ (which is rigorously true among all convex bodies) and the simplices bound $B_2(K)/v(K)$ from above, provided that the convex bodies are sufficiently compact, as shown in figure 8. Consistent with observations made in section 6.2, if the aspect ratio $h/a$ is sufficiently large at fixed $d$, $B_2(K)/v(K)$ for spherocylinders can exceed that for simplices.



J. Stat. Mech. (2022) 093404

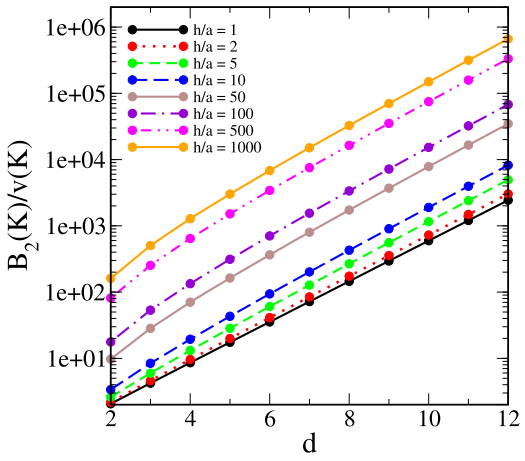



**Figure 9.** Dimensionless second virial coefficient $B_2(K)/v(K)$ for randomly oriented spherocylinders at selected aspect ratios $h/a \in [1, 1000]$ in dimensions $d = 2$ to 12.

### 6.3. Percolation thresholds across dimensions

In our previous work [9], we showed the scaling relation (5), which depends on the ratio $v_{\rm ex}(K)/v(K)$, provides reasonably accurate estimates of the percolation threshold $\eta_{\rm c}$ of many different overlapping convex bodies in two and three dimensions when compared to corresponding simulation data. It follows from the analysis given there that the general scaling relation (5) must become increasingly accurate as $d$ becomes large for a given convex body. This is yet another manifestation of the principle that low-dimensional percolation properties encode high-dimensional information [7]. In light of the fact that the formula for dimensionless exclusion volume $v_{\rm ex}(K)/v(K)$ given in [9] of a convex body is generally a lower bound on this quantity for $d \geqslant 4$ (see section 3.3), this means that the scaling estimates for $\eta_{\rm c}$ for the selected convex shapes given there were generally overestimated for $d \geqslant 4$. Thus, our interest here is in evaluating the accurate scaling relation (5) across dimensions using the exact expressions for $v_{\rm ex}(K)/v(K)$ for the aforementioned convex bodies given in the present paper.

While we expect the scaling relation (5) to be already very accurate for $d = 4$ and greater dimensions, we confirm this expectation by carrying out computer simulations of the percolation threshold $\eta_{\rm c}$ for spherocylinders and regular simplices for dimensions 2 through 5 using the rescaled-particle simulation method discussed in detail in [8]. Spherocylinders are centrally symmetric bodies and allow us to investigate the effects of elongation on the theoretical estimates of $\eta_{\rm c}$ based on the scaling relation across dimensions, which is a challenging case to predict. We chose to simulate percolation of simplices because they are compact, noncentrally symmetric bodies.

Figure 10 compares the rescaled-particle simulation results for simplices to the scaling relation (5) as well as to the lower bound (4). Figure 11 shows the corresponding plot for spherocylinders. A crucial observation to be made from the figures is how closely the scaling relation (5) predicts the simulated values of $\eta_{\rm c}$ for the both simplices and spherocylinders across the relatively low dimensions from $d = 2$ through $d = 5$. For



J. Stat. Mech. (2022) 093404

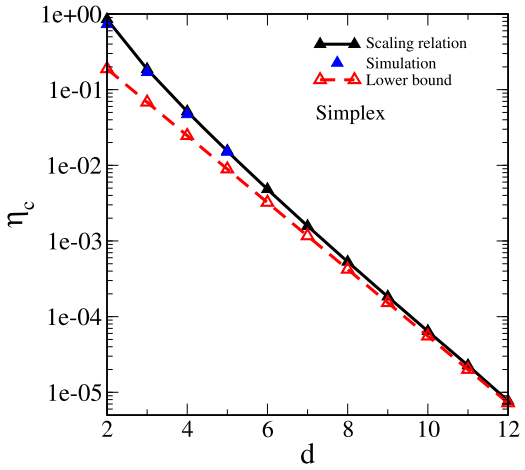



**Figure 10.** Percolation threshold $\eta_c$ for systems of randomly oriented simplices in dimensions $d = 2$ to 12 obtained using scaling relation (5), which is compared to the simulation data and lower bound (4).

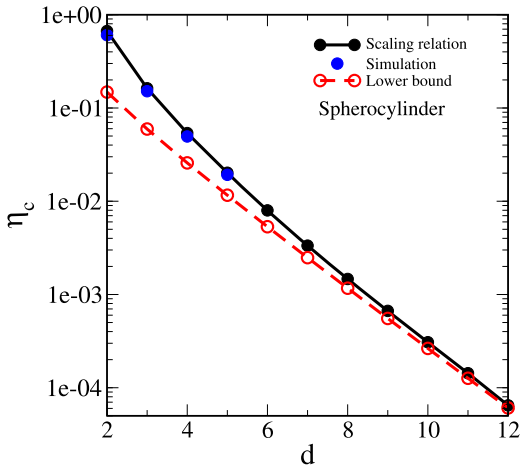



**Figure 11.** Percolation threshold $\eta_c$ for systems of randomly oriented spherocylinders with $h/a = 10$ in dimensions $d = 2$ to 12 obtained using scaling relation (5), which is compared to the simulation data and lower bound (4).

reasons noted earlier, the scaling relation will yield analytical predictions with increasing accuracy as $d$ increases and becomes exact in $d \to \infty$. This can also be seen from the convergence of the scaling relation prediction and the rigorous lower bound, the latter of which becomes exact in the high-$d$ limit [9]. Using the high-$d$ scalings reported in section 6.1 together with scaling relation (5) enables us to conclude that the decay of $\eta_c$ with $d$ is controlled by the inverse power law $2^{-1.6618d}$ for simplices and the inverse power law $2^{-d}$ for spherocylinders.

Having further verified the accuracy of the scaling relation for simplices and spherocylinders, we now employ it to predict $\eta_c$ for other shapes. Figure 12 shows such estimates



J. Stat. Mech. (2022) 093404

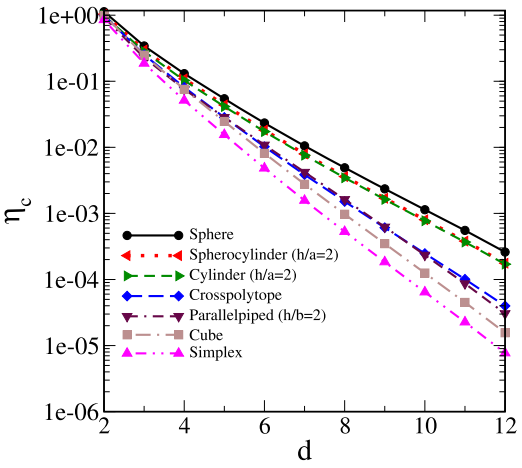



**Figure 12.** Percolation threshold $\eta_c$ for systems of randomly oriented convex bodies for selected shapes, including the sphere, spherocylinder, cylinder, cube, parallelpiped, cross-polytope, and simplex in dimensions $d = 2$ to 12, as obtained from scaling relation (5).

of $\eta_c$ for selected convex bodies across dimensions. Since $\eta_c$ is inversely proportional to the dimensionless exclusion volume $v_{ex}(K)/v(K)$ (cf equation (5)), the behavior of $\eta_c$ for different shapes at fixed $d$ is the opposite of the trends described in section 6.1 for the corresponding $v_{ex}(K)/v(K)$. For example, among the compact shapes with finite volumes, spheres possess the largest threshold $\eta_c$, and simplices possess the smallest value of $\eta_c$, whether they are randomly oriented or uniformly oriented. In fact, according to the rigorous relations (77) and (86) and [7], the sphere provably possesses the maximal threshold among all such nonzero-volume convex bodies in the high-$d$ limit. Thus, we conjecture that overlapping spheres possess the maximal value of $\eta_c$ among all identical nonzero-volume convex overlapping bodies, randomly or uniformly oriented, for $d \geqslant 2$. Furthermore, in light of the upper bound (77), we conjecture that among all oriented nonzero-volume convex bodies, overlapping simplices have the minimal value of $\eta_c$ for $d \geqslant 2$.

While randomly oriented simplices yield the lowest percolation thresholds among the convex bodies considered, provided that they are relatively compact, elongated shapes, such as spherocylinders, can have a lower threshold if their aspect ratio $h/a$ is sufficiently large. These distinctions between the percolation thresholds of these two convex bodies are clearly seen in figure 13. Consistent with the results reported in section 6.1, we see that for a fix aspect ratio $h/a$, there is a crossover dimension $d^* \sim \ln(h/a)$ beyond which the simplices possess smaller values of $\eta_c$ compared to that of spherocylinders. We also see from figure 12 that cubes possess a smaller value of $\eta_c$ than that of cross-polytopes; and cylinders possess a smaller value of $\eta_c$ than that of spherocylinders with the same aspect ratio. In the case of cubes, exact high-$d$ asymptotic formula (45) reported together with scaling relation (5) enables us to conclude that the decay of $\eta_c$ with $d$ is controlled by the inverse power law $2^{-3d/2}$.



J. Stat. Mech. (2022) 093404

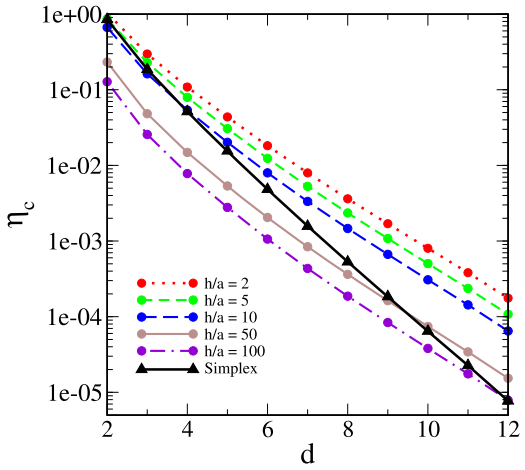



**Figure 13.** Comparison of the percolation threshold $\eta_c$ for randomly oriented spherocylinders with various aspect ratios $h/a$ to that of randomly oriented simplices across dimensions, as obtained using the scaling relation (5).

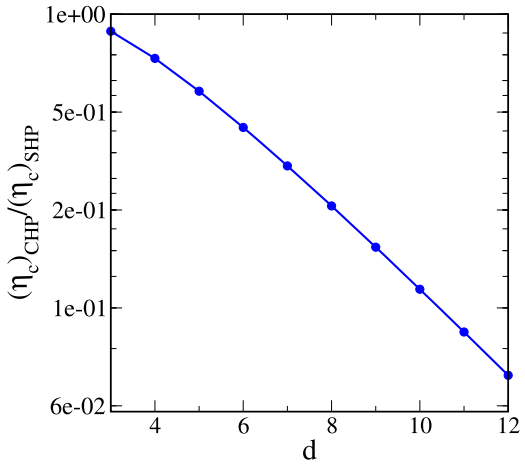



**Figure 14.** Ratio between the percolation threshold of cubical hyperplates $(\eta_c)_{\,\mathrm{CHP}}$ and that of spherical hyperplates $(\eta_c)_{\,\mathrm{SHP}}$ dimensions $d = 3$ to 12 obtained using the scaling relation (7).

Figure 14 shows the ratio between the percolation threshold of cubical hyperplates $(\eta_c)_{\,\mathrm{CHP}}$ and that of spherical hyperplates $(\eta_c)_{\,\mathrm{SHP}}$ in dimensions $d = 3$ to 12 obtained using the scaling relation (7). In principle, the scaling relation (7) allows one to obtain accurate estimates of the percolation threshold for nonspherical hyperplates, given accurate values of $(\eta_c)_{\,\mathrm{SHP}}$ for the reference spherical hyperplate system. However, such values are not available, except for $d = 3$ [28]. In [9], we showed that equation (7) indeed led to very accurate estimates of the percolation thresholds for various two-dimensional plates in three-dimensional space, including square, triangular, elliptical and rectangular plates. Such good agreement already for $d = 3$ means that the scaling relation (7) should become increasingly more accurate as $d$ increases above three. Figure 14 shows

J. Stat. Mech. (2022) 093404

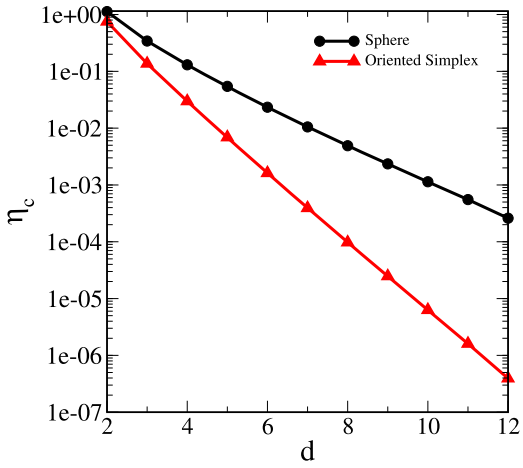



**Figure 15.** Percolation threshold $\eta_c$ for uniformly oriented simplices and spheres in dimensions $d = 2$ to 12, as obtained using the scaling relation (5).

the percolation threshold of cubical hyperplates relative to that of spherical hyperplates descends exponentially fast with $d$, namely, it decays like $2^{-d/2}$, which is obtained using the high-$d$ scalings reported in section 4 together with scaling relation (7). In analogy with the conjectures made above for full $d$-dimensional bodies, we conjecture that among all the convex hyperplates, spherical hyperplates have the largest percolation thresholds for any fixed $d \geqslant 3$. We emphasize again that in general, results for $(d-1)$-dimensional bodies should not be compared to those for full $d$-dimensional bodies, especially because of the arbitrary choice used for the effective volume $v_{\rm eff}(K_{\rm H})$ of a zero-volume hyperplate in (7) to make its exclusion volume dimensionless, as stressed in section 6.1.

Finally, we note that randomly oriented non-spherical hyperparticles generally have a much smaller threshold than that of their oriented counterparts due to the theorems presented in section 5. This can be seen by comparing the curves of $\eta_c$ of oriented simplices, which must decay like $2^{-2d}$, shown in figure 15 to that of $\eta_c$ of randomly oriented simplices, which decays like $2^{-1.6618}$, shown in figure 12. Figure 15 also includes the estimate of $\eta_c$ for spheres.

## 7. Conclusions

In this paper, we have provided a general formula for the exclusion volume $v_{\rm ex}(K)$ for an arbitrary convex body $K$ in any space dimension, including both the rotationally-averaged exclusion volume and the exclusion volume associated with uniform orientations of $K$. We showed that the sphere minimizes the dimensionless exclusion volume $v_{\rm ex}(K)/v(K)$ among all convex bodies, whether randomly oriented or uniformly oriented, for any $d$. When the bodies have the same orientation, the simplex maximizes the dimensionless exclusion volume $v_{\rm ex}(K)/v(K)$ for any $d$ with a large-$d$ asymptotic scaling behavior of $2^{2d}/d^{3/2}$. We demonstrated that the rotationally-averaged exclusion volume $v_{\rm ex}(K)$ can be written as certain weighted sums of quermassintegrals $W_0(K), \ldots, W_d(K)$



J. Stat. Mech. (2022) 093404

of $K$. Subsequently, we presented explicit expressions for quermassintegrals for various nonspherical convex bodies, including cubes, parallelepipeds, regular simplices, cross-polytopes, cylinders, spherocylinders, ellipsoids as well as lower-dimensional bodies, such as hyperplates and line segments. For certain shapes, explicit formula and large-$d$ asymptotic expressions of $v_{\rm ex}(K)$ are obtained. These results were used to evaluate the rotationally-averaged ratio $v_{\rm ex}(K)$ for these convex-body shapes for dimensions 2 through 12. While the sphere is the minimal shape, we showed that among the convex bodies considered that are sufficiently compact, the simplex possesses the maximal $v_{\rm ex}(K)/v(K)$ with a scaling behavior of $2^{1.6618\ldots d}$, which grows more slowly than the corresponding ratio for oriented simplices.

The exclusion volume results were subsequently utilized to determine the corresponding second virial coefficient $B_2(K)/v(K)$ of the hard hyperparticles that we considered for the first time. Such information allows us to draw some conclusions on the effect of body shape on the disorder–order equilibrium phase transition in relatively low dimensions for several reasons. First, we have demonstrated that the scaling behavior of $v_{\rm ex}(K)/v(K)$ or, equivalently, $B_2(K)/v(K)$ for a range of relatively low dimensions considered (from $d=6$ to $d=12$) agrees well with the exact high-$d$ asymptotic scalings. This further supports the general principle that high-dimensional information is encoded in relatively low dimensions [7–9]. Second, we noted earlier that the dominant contribution to the pressure of a hard-hyperparticle equilibrium fluid is given by the truncation of the virial expansion through second-order terms (cf (2)) in the high-$d$ asymptotic limit [21]. Thus, in sufficiently high dimensions, we expect that hyperparticles with a larger dimensionless exclusion volume $v_{\rm ex}(K)/v(K)$ should have an entropy-driven disorder–order transition occurring at a lower density, since hyperparticles with larger exclusion volumes impose non-trivial correlations among their neighbors at much lower densities than those with smaller exclusion volumes. The same idea was used by Onsager to discover a nematic phase transition for needle-like particles in three dimensions [11].

We also applied our results to compute estimates of the continuum percolation threshold $\eta_{\rm c}$ using a scaling relation derived previously by the authors for systems of identical overlapping convex bodies. It is noteworthy that while the scaling relation becomes exact in $d\to\infty$, it already yields very accurate predictions even in relatively low dimensions. The accuracy of the scaling relation predictions is ascertained using numerical simulations for simplices and spherocylinders in dimensions 2 through 5, which verify that these estimates indeed become increasingly accurate as the space dimension increases. Among the shapes with nonzero volume that we examined, we showed that spheres possess the largest threshold $\eta_{\rm c}$, and simplices possess the smallest value of $\eta_{\rm c}$, whether they are randomly oriented or uniformly oriented. We conjectured that overlapping spheres possess the maximal value of $\eta_{\rm c}$ among all identical nonzero-volume convex overlapping bodies, randomly or uniformly oriented, for $d\geqslant 2$. We also conjectured that, among all identical, oriented nonzero-volume convex bodies, overlapping simplices have the minimal value of $\eta_{\rm c}$ for $d\geqslant 2$. Similarly, we conjecture that among all the convex hyperplates, spherical hyperplates have the largest percolation thresholds for any fixed $d\geqslant 3$.

J. Stat. Mech. (2022) 093404

It should not go unnoticed that the scaling relations for $\eta_c$ that utilize the exact general explicit expressions for the exclusion volume readily allow one to estimate the percolation threshold of a wide spectrum of hyperparticles across dimensions, well beyond the specific choices of shape parameters and dimensions that we explicitly studied here. Importantly, our numerical results indicate that the estimates of $\eta_c$ are already reasonably accurate in three dimensions, which opens up many practical applications of our results in physics and material science problems that account for the effect of particle shapes.

In the introduction, we noted the duality relation between the continuum percolation of overlapping hyperparticles and the equilibrium hard-hyperparticle fluids of the same shape [7]. Combination of this duality relation with the so-called decorrelation principle for disordered hard-hyperparticle packings [29, 30], implies that in sufficiently high dimensions the percolation threshold $\eta_c$ of overlapping hyperparticles is directly related to the disorder–order phase transition density (i.e. the freezing-point) of the corresponding equilibrium hard-hyperparticle fluid [7]. This is an outstanding open problem for future research.

Finally, we note that our results for the dimensionless oriented exclusion volume $v_{ex}^o(K)/v(K)$ of convex body $K$ has implications for the optimal packing of $K$ [15]. Specifically, it has been conjectured [31] that the optimal packing of a centrally symmetric convex body with equivalent principal axes (e.g. an octahedron) is achieved by the associated optimal Bravais-lattice packing in which all the bodies are aligned; while the optimal packing of a body without central symmetry (e.g. a tetrahedron) is generally given by a non-Bravais-lattice packing in which the bodies have different orientations. Our current study further supports these organizing principles, i.e. $v_{ex}^o(K)/v(K)$ is minimized when the bodies are aligned for a centrally symmetric body, while nonaligned orientations can result in a much smaller $v_{ex}^o(K)/v(K)$ for noncentrally symmetric shapes. Moreover, our new results on the exclusion volumes for a wide spectrum of convex bodies across dimensions suggest that similar organizing principles for the densest packings could also hold in higher dimensions ($d \geqslant 4$), which we will explore in our future studies.

## Acknowledgments

We are deeply grateful to Yair Shenfeld who made us aware of the relationship of quermassintegrals to exclusion volumes and how our previous expression for the latter is a lower bound. We thank Alexander McWeeney for his assistance with preliminary calculations using the rescaled particle method. This work was supported by the National Science Foundation under Grant No. CBET-1701843.

## Appendix A. Quermassintegrals of lower-dimensional bodies and hyperplates

As discussed in the introduction, it is also of interest to consider lower-dimensional bodies and hyperplates in $\mathbb{R}^d$. These bodies in $\mathbb{R}^d$ have zero volume, and so an effective



J. Stat. Mech. (2022) 093404

volume (6) is used in the bound (4). The exclusion volume of a hyperplate, however, is defined exactly as in section 2, and the formula (21) still applies. Thus to calculate the exclusion volume of a hyperplate, we must be able to calculate its quermassintegrals. It turns out that there is a very general way to find the quermassintegrals of a low-dimensional body in $\mathbb{R}^d$. By a low-dimensional body, we mean a body whose intrinsic dimension is $(d-1)$ or less.

### A.1. Intrinsic volumes

The quermassintegrals of a body $K \subset \mathbb{R}^d$ measure the cross-sectional volumes of $K$ in $\mathbb{R}^d$, which was explained in some detail in section 3.3. Intuitively, the cross-sectional volumes of a body $K$ should be the same regardless of the dimension of the ambient space $\mathbb{R}^d$ in which $K$ is embedded. However, the quermassintegrals of a body do actually depend on the dimension of the embedding space: nevertheless, there is a normalization of the quermassintegrals, called the *intrinsic volumes* or Minkowski functionals, which is invariant with respect to the dimension of the embedding space.

To be more precise, fix a body $K$ and an embedding space $\mathbb{R}^d$. We have already defined the quermassintegrals $W_0(K), \ldots, W_d(K)$. We now define a new set of functions, $V_0(K), \ldots, V_d(K)$, called the *intrinsic volumes* of $K$, in the following manner [18]:

$$V_i(K) = \frac{1}{\kappa_{d-i}} \binom{d}{i} W_{d-i}(K), \tag{A.1}$$

where $\kappa_{d-i}$ is the volume of the unit sphere in $\mathbb{R}^{d-i}$, defined in relation (40); we take the additional convention that $\kappa_0 = 1$. This definition makes $V_i$ a measure of the $i$-dimensional cross-sectional volume of $K$.

As it turns out, the definition we have given for the functions $V_i$ does not depend on the definition of the ambient space. That is, suppose $K$ is a body in $\mathbb{R}^d$, with intrinsic volumes $V_0(K), \ldots, V_d(K)$ with respect to $\mathbb{R}^d$. Now place $K$ into the space $\mathbb{R}^D$ with $D > d$, and let $V_0'(K), \ldots V_d'(K), \ldots, V_D'(K)$ be the intrinsic volumes of $K$ with respect to $\mathbb{R}^D$. Then, for $0 \leqslant i \leqslant d$, we have $V_i(K) = V_i'(K)$.

Using this fact, we can find the quermassintegrals of a body in a lower dimensional space to calculate its quermassintegrals in a higher dimensional space. Let $K$ be a convex body in $\mathbb{R}^d$, with quermassintegrals $W_0', \ldots, W_d'$ and intrinsic volumes $V_0, \ldots, V_d$. We want to calculate the quermassintegrals $W_0, \ldots, W_D$ for $K$ embedded in $\mathbb{R}^D$ for $D > d$.

To do this, we first note the following: if $K$ can be embedded in $\mathbb{R}^d$, then $K$ is at most $d$-dimensional. In $\mathbb{R}^D$, this means that $V_i(K) = 0$ for $d < i \leqslant D$. This follows formally from equation (4.23) of [18]; intuitively, this follows from the idea that if $K$ is at most $d$-dimensional, then its cross-sectional volumes of dimension greater than $d$ should be 0.

We now have the following from relation (A.1):

$$W_i(K) = \kappa_i \binom{D}{D-i}^{-1} V_{D-i}(K). \tag{A.2}$$



J. Stat. Mech. (2022) 093404

Thus, if $D-i>d$, then $W_i(K)=0$. If $D-i\leqslant d$, then

$$\begin{aligned} W_i(K) &= \kappa_i \binom{D}{D-i}^{-1} V_{D-i}(K) \\ &= \kappa_i \binom{D}{D-i}^{-1} \left( \frac{1}{\kappa_{d-D+i}} \binom{d}{d-D+i} W'_{d-D+i}(K) \right) \\ &= \frac{\kappa_i}{\kappa_{d-D+i}} \binom{D}{D-i}^{-1} \binom{d}{d-D+i} W'_{d-D+i}(K). \end{aligned} \tag{A.3}$$

In summary, we have

$$W_i(K) = \begin{cases} \dfrac{\kappa_i}{\kappa_{d-D+i}} \binom{D}{D-i}^{-1} \binom{d}{d-D+i} W'_{d-D+i}(K) & D-i\leqslant d \\ 0 & D-i>d. \end{cases} \tag{A.4}$$

### A.2. Application to spherical hyperplates

Here, we apply formula (A.4) to spherical hyperplates. A spherical hyperplate is a $(d-1)$-dimensional sphere in $\mathbb{R}^d$. Suppose we have a spherical hyperplate $H$ of radius $a$. Then, in $\mathbb{R}^{d-1}$, we have

$$W'_i(H) = \kappa_{d-1} a^{d-1-i}. \tag{A.5}$$

Thus, in $\mathbb{R}^d$, we have $W_0(H)=0$, and for $i\geqslant 1$

$$\begin{aligned} W_i(H) &= \frac{\kappa_i}{\kappa_{i-1}} \binom{d}{d-i}^{-1} \binom{d-1}{i-1} W'_{i-1}(H) \\ &= \left( \frac{\kappa_{d-1}}{\kappa_{i-1}} \cdot \frac{i}{d} \right) \kappa_i a^{d-i}. \end{aligned} \tag{A.6}$$

It is interesting to observe that if $C$ is a cube with edge length $a$, then the above formula says that

$$W_i(H) = \left( \frac{\kappa_{d-1}}{\kappa_{i-1}} \cdot \frac{i}{d} \right) W_i(C). \tag{A.7}$$



J. Stat. Mech. (2022) 093404

### A.3. Application to cubical hyperplates

We now apply (A.4) to cubical hyperplates. A cubical hyperplate is a $(d-1)$-dimensional cube in $\mathbb{R}^d$. Suppose we have a cubical hyperplate $H$ with edge length $b$. Then, in $\mathbb{R}^{d-1}$, we have

$$W_i'(H) = \kappa_i b^{d-1-i}. \tag{A.8}$$

Thus, in $\mathbb{R}^d$, we have $W_0(H) = 0$, and for $i \geqslant 1$

$$\begin{aligned} W_i(H) &= \frac{\kappa_i}{\kappa_{i-1}} \binom{d}{d-i}^{-1} \binom{d-1}{i-1} W_{i-1}'(H) \\ &= \left(\frac{i}{d}\right) \kappa_i b^{d-i}. \end{aligned} \tag{A.9}$$

Once again, we observe that if $C$ is a cube of edge length $b$, then the above formula says that

$$W_i(H) = \left(\frac{i}{d}\right) W_i(C). \tag{A.10}$$

Furthermore, if $H_{\mathrm{S}}$ is a spherical hyperplate of radius $a$, then

$$W_i(H) = \left(\frac{\kappa_{d-1}}{\kappa_{i-1}}\right)^{-1} W_i(H_{\mathrm{S}}). \tag{A.11}$$

### A.4. Dimensionless exclusion volume for selected shapes across dimensions

In the main paper, we graphically show the dimensionless exclusion volume $v_{\mathrm{ex}}(K)/v(K)$ for selected shapes in dimensions 2 through 12. Here, we provide the values for these shapes, which are provided in Tables A1–A4.

J. Stat. Mech. (2022) 093404

**Table A1.** Values of dimensionless exclusion volume $v_{ex}(K)/v(K)$ for selected shapes in dimensions 2 through 12. The aspect ratio of the cylinder and parallelpiped are respectively are $h/a = 2$ and $h/b = 2$.

| | Sphere | Cylinder | Cross-polytope | Parallelpiped | Cube | Simplex |
|---|---|---|---|---|---|---|
| $d = 2$ | 4 | 4.546 48 | 4.546 48 | 4.864 79 | 4.546 48 | 5.307 97 |
| $d = 3$ | 8 | 9.712 39 | 10.8301 | 12 | 11 | 14.6726 |
| $d = 4$ | 16 | 20.3032 | 25.7981 | 27.5211 | 27.5812 | 40.5589 |
| $d = 5$ | 32 | 42.0105 | 61.453 | 61.25 | 70.75 | 112.115 |
| $d = 6$ | 64 | 86.4313 | 146.386 | 137.647 | 184.352 | 309.916 |
| $d = 7$ | 128 | 177.184 | 348.702 | 319.417 | 485.875 | 856.69 |
| $d = 8$ | 256 | 362.325 | 830.635 | 770.823 | 1291.69 | 2368.11 |
| $d = 9$ | 512 | 739.563 | 1978.64 | 1928.83 | 3457.3 | 6546.0 |
| $d = 10$ | 1024 | 1507.39 | 4713.27 | 4968.09 | 9304.28 | 18095.1 |
| $d = 11$ | 2048 | 3068.79 | 11227.4 | 13069.1 | 25 152 | 50019.5 |
| $d = 12$ | 4096 | 6241.36 | 26744.5 | 34886.3 | 68247.7 | 138267 |

**Table A2.** Values of dimensionless exclusion volume $v_{ex}(K)/v(K)$ for spherocylinders with selected aspect ratios $h/a$ in dimensions 2 through 12.

| | $h/a = 1$ | $h/a = 2$ | $h/a = 10$ | $h/a = 50$ | $h/a = 100$ | $h/a = 500$ | $h/a = 1000$ |
|---|---|---|---|---|---|---|---|
| $d = 2$ | 4.123 82 | 4.356 57 | 6.750 98 | 19.4307 | 35.3387 | 162.657 | 321.811 |
| $d = 3$ | 8.428 57 | 9.2 | 16.8235 | 56.7013 | 106.684 | 506.67 | 1006.67 |
| $d = 4$ | 17.1691 | 19.205 | 38.781 | 140.393 | 267.683 | 1286.25 | 2559.48 |
| $d = 5$ | 34.9032 | 39.8261 | 86.2169 | 325.734 | 625.668 | 3025.61 | 6025.61 |
| $d = 6$ | 70.8532 | 82.2191 | 187.671 | 729.985 | 1408.92 | 6841.3 | 13631.9 |
| $d = 7$ | 143.672 | 169.176 | 402.869 | 1601.06 | 3100.82 | 15100.6 | 30100.6 |
| $d = 8$ | 291.067 | 347.206 | 856.329 | 3460.44 | 6719.46 | 32 795 | 6389.9 |
| $d = 9$ | 589.233 | 711.097 | 1806.77 | 7400.04 | 14399.1 | 70398.4 | 140 398 |
| $d = 10$ | 1192.07 | 1453.86 | 3790.24 | 15697.6 | 30596.4 | 149 799 | 298 805 |
| $d = 11$ | 2410.32 | 2968.11 | 7914.57 | 33089.3 | 64 586 | 316 583 | 631 583 |
| $d = 12$ | 4871.15 | 6051.91 | 16464.4 | 69395.1 | 15 613 | 665 405 | 1327 650 |

J. Stat. Mech. (2022) 093404

**Table A3.** Values of dimensionless exclusion volume $v_{\rm ex}(K_{\rm H})/v_{\rm eff}(K_H)$ for spherical and cubical hyperplates in dimensions 3 through 12.

| | Spherical hyperplate | Cubical hyperplate |
|---|---|---|
| $d = 3$ | 2.356 19 | 2.658 68 |
| $d = 4$ | 5.548 69 | 7.589 25 |
| $d = 5$ | 12.1491 | 20.9595 |
| $d = 6$ | 25.7115 | 57.3242 |
| $d = 7$ | 53.4209 | 156.398 |
| $d = 8$ | 109.785 | 426.778 |
| $d = 9$ | 224.059 | 1165.98 |
| $d = 10$ | 455.162 | 3190.45 |
| $d = 11$ | 921.644 | 8744.25 |
| $d = 12$ | 1861.86 | 24004.1 |

**Table A4.** Values of dimensionless exclusion volume $v_{\rm ex}^0(K)/v(K)$ for oriented simplices in dimensions 2 through 12.

| | Oriented simplex |
|---|---|
| $d = 2$ | 4 |
| $d = 3$ | 8 |
| $d = 4$ | 16 |
| $d = 5$ | 32 |
| $d = 6$ | 64 |
| $d = 7$ | 128 |
| $d = 8$ | 256 |
| $d = 9$ | 512 |
| $d = 10$ | 1024 |
| $d = 11$ | 2048 |
| $d = 12$ | 4096 |

## References


[1] Kihara T 1953 Virial coefficients and models of molecules in gases *Rev. Mod. Phys.* **25** 831–43
[2] Luban M and Baram A 1982 Third and fourth virial coefficients of hard hyperspheres of arbitrary dimensionality *J. Chem. Phys.* **76** 3233–41
[3] Hansen J P and McDonald I R 1986 *Theory of Simple Liquids* (New York: Academic)
[4] Tarjus G, Viot P, Ricci S M and Talbot J 1991 New analytical and numerical results on virial coefficients for 2D hard convex bodies *Mol. Phys.* **73** 773–87
[5] Balberg I, Anderson C H, Alexander S and Wagner N 1984 Excluded volume and its relation to the onset of percolation *Phys. Rev.* B **30** 3933–43
[6] Bug A L R, Safran S A, Grest G S and Webman I 1985 Do interactions raise or lower a percolation threshold? *Phys. Rev. Lett.* **55** 1896–9
[7] Torquato S 2012 Effect of dimensionality on the continuum percolation of overlapping hyperspheres and hypercubes *J. Chem. Phys.* **136** 054106


J. Stat. Mech. (2022) 093404

[8] Torquato S and Jiao Y 2012 Effect of dimensionality on the continuum percolation of overlapping hyperspheres and hypercubes: II. Simulation results and analyses *J. Chem. Phys.* **137** 074106
[9] Torquato S and Jiao Y 2013 Effect of dimensionality on the percolation threshold of overlapping nonspherical hyperparticles *Phys. Rev.* E **87** 022111
[10] Onsager L 1944 Crystal statistics: I. A two-dimensional model with an order–disorder transition *Phys. Rev.* **65** 117–49
[11] Onsager L 1949 The effects of shape on the interaction of colloidal particles *Ann. New York Acad. Sci.* **51** 627–59
[12] Frenkel D 1987 Onsager's spherocylinders revisited *J. Phys. Chem.* **91** 4912–6
[13] Perram J W and Wertheim M S 1985 Statistical mechanics of hard ellipsoids: I. Overlap algorithm and the contact function *J. Comput. Phys.* **58** 409–16
[14] Donev A, Torquato S and Stillinger F 2005 Neighbor list collision-driven molecular dynamics simulation for nonspherical hard particles: II. Applications to ellipses and ellipsoids *J. Comput. Phys.* **202** 765–93
[15] Torquato S and Jiao Y 2009 Dense packings of the platonic and Archimedean solids *Nature* **460** 876–9
[16] Santaló L A 1976 *Integral Geometry and Geometric Probability Encyclopedia of Mathematics and its Applications* (Reading, MA: Addison-Wesley Developers Press)
[17] Stoyan D, Kendall W S and Mecke J 1995 *Stochastic Geometry and its Applications* 2nd edn (New York: Wiley)
[18] Schneider R 2014 *Convex Bodies: The Brunn–Minkowski Theory Encyclopedia of Mathematics and its Applications* (Cambridge: Cambridge University Press)
[19] Mecke K R 2000 Additivity, convexity, and beyond: applications of Minkowski functionals in statistical physics *Statistical Physics and Spatial Statistics* (Berlin: Springer) pp 111–84
[20] Coxeter H S M 1973 *Regular Polytopes* (New York: Dover)
[21] Frisch H L and Percus J K 1999 High dimensionality as an organizing device for classical fluids *Phys. Rev.* E **60** 2942–8
[22] Quintanilla J, Torquato S and Ziff R M 2000 Efficient measurement of the percolation threshold for fully penetrable discs *J. Phys. A: Math. Gen.* **33** L399–407
[23] Rintoul M D and Torquato S 1997 Precise determination of the critical threshold and exponents in a three-dimensional continuum percolation model *J. Phys. A: Math. Gen.* **30** L585–92
[24] Lorenz C D and Ziff R M 2000 Precise determination of the critical percolation threshold for the three-dimensional 'Swiss cheese' model using a growth algorithm *J. Chem. Phys.* **114** 3659
[25] Hug D and Weil W 2020 *Lectures on Convex Geometry* (Berlin: Springer)
[26] Zaporozhets D and Kabluchko Z 2014 Random determinants, mixed volumes of ellipsoids, and zeros of Gaussian random fields *J. Math. Sci.* **199** 168–73
[27] Henk M, Richter-Gebert J and Ziegler G M 1997 Basic properties of convex polytopes *Handbook of Discrete and Computational Geometry* (Boca Raton, FL: CRC Press)
[28] Yi Y B and Tawerghi E 2009 Geometric percolation thresholds of interpenetrating plates in three-dimensional space *Phys. Rev.* E **79** 041134
[29] Torquato S and Stillinger F H 2006 New conjectural lower bounds on the optimal density of sphere packings *Exp. Math.* **15** 307
[30] Zachary C E and Torquato S 2011 High-dimensional generalizations of the Kagomé and diamond crystals and the decorrelation principle for periodic sphere packings *J. Stat. Mech.* P10017
[31] Torquato S and Jiao Y 2012 Organizing principles for dense packings of nonspherical hard particles: not all shapes are created equal *Phys. Rev.* E **86** 011102

J. Stat. Mech. (2022) 093404